Signal Processing 90 (2010) 3164–3184

Contents lists available at ScienceDirect

Signal Processing

journal homepage: www.elsevier.com/locate/sigpro

On the statistics of matching pursuit angles

Lisandro Lovisolo [a,*], Eduardo A.B. da Silva [b], Paulo S.R. Diniz [b]

[a] PROSAICO–PEL/DETEL–UERJ, Rio de Janeiro, RJ, Brasil
[b] LPS–COPPE/UFRJ, Cx. P. 68504, Rio de Janeiro, RJ, Brasil

ARTICLE INFO

Article history:
Received 27 March 2009
Received in revised form
9 March 2010
Accepted 17 May 2010
Available online 26 May 2010

Keywords:
Source coding
Overcomplete representations
Matching pursuits
Lloyd–Max quantization

ABSTRACT

Matching pursuit decompositions have been employed for signal coding. For this purpose, matching pursuit coefficients need to be quantized. However, their behavior has been shown to be chaotic in some cases; posing difficulties to their modeling and quantizer design. In this work, a different approach is presented. Instead of trying to model the statistics of matching pursuit coefficients, the statistics of the angle between the residue signal and the element selected in each iteration of the matching pursuit are studied, what allows to model matching pursuits coefficients indirectly. This approach results in a simple statistical model. This is so because one observes that the statistics of such angles do not vary substantially after the first matching pursuit iteration, and can be approximately modeled as independent and identically distributed. Moreover, it is also observed that the probability density functions of matching pursuit angles are reasonably modeled by a single probability density function. This function depends only on the dictionary employed and not on the signal source. The derived statistical model is validated by employing it to design Lloyd–Max quantizers for matching pursuit coefficients. The Lloyd–Max quantizers obtained show good rate $\times$ distortion performance when compared to the state-of-the-art methods.

1. Introduction

The Matching Pursuit algorithm (MP) [1,2] is a technique to decompose a signal through a weighted sum of atoms which are selected utilizing a greedy criterion. It employs an overcomplete collection of predefined elements or atoms; this collection is the so-called dictionary and is overcomplete because it contains more elements than necessary to span the signal space [1–4].

The MP has been used for: signal filtering and denoising [5,2,6]; analysis of the physical phenomena underlying the signals associated with pattern recognition and signal modeling [5,2,7–12]; time-frequency [1,2] and harmonic analyses [12,13]. It has been also employed for signal compression [5,13–19].

The MP starts by searching the dictionary atom that has the largest inner product with the signal. The signal is first approximated by the selected atom scaled by its inner product with the signal. The approximation error or residue is the difference between the signal and the scaled atom. To improve the approximation, the same process is applied to the residue and iterated until a given approximation error norm or a given number of atoms is reached. Since this algorithm searches for the best possible approximation in each iteration it is said to be greedy.

The MP has been used in different flavors of encoding algorithms. In some cases its usage resembles gain-shape vector quantization as it is used for extracting very few atoms highly correlated with the signal and correspondent coefficients [5,20]. In a similar framework it was used to encode video residues [21,22]. When the MP is used for encoding the coefficients obtained in the decomposition must be quantized and transmitted along with atom indices. Some works employ in-loop

* Corresponding author.
E-mail addresses: lisandro@uerj.br (L. Lovisolo), eduardo@lps.ufrj.br (E.A. da Silva), diniz@lps.ufrj.br (P.S.R. Diniz).

0165-1684/$ - see front matter © 2010 Elsevier B.V. All rights reserved.
doi:10.1016/j.sigpro.2010.05.021

quantization [15–17], i.e, the quantization is considered before computing the residue; others use off-loop (or open-loop) quantization [18,5]. Quantizers providing good rate-distortion behavior are required. However, for designing such quantizers statistical models are required.

Although the MP has been present in the literature for over ten years a full understanding of the statistical properties of MP residues and coefficients is not available. In this work we address this issue by analyzing the statistics of the angles between residues and the atoms selected in MP iterations. We have verified that such statistics, after the first stage, have the asymptotic tendency to depend only on the dictionary used, being approximately independent of the signal being decomposed. That is, we report that these statistics can be modeled as depending only on the dictionary, after some initial decomposition steps and not on the source. Therefore, for some applications there might be no need to indicate the source being decomposed and the same quantizer might be used for any source and this has been verified in the MP coefficients quantization application. That is, the observed result is employed to design an off-loop Lloyd–Max quantizer for the coefficients of MP decompositions. This quantizer, when applied to code MP decompositions and compared to state-of-the-art quantization schemes for MP coefficients validates the adequacy of the statistical model.

Organization and main results—Off-loop quantization of MP coefficients is discussed in Section 2, along with the pros and cons of this coding framework for MP based encoders. In Section 3, MP coefficients are expressed using the angles between residues and atoms in Matching Pursuit iterations. In Section 4, we observe that, for outcomes of a signal source whose probability density function depends of only the signal energy, the statistics of MP angles are asymptotically independent of the iteration. It is also observed that for other signal sources, whose corresponding probability density functions do not depend only on the magnitude of the outcome but also on its angle, the same behavior is observed after some Matching Pursuit iterations. As a result, since the orientation of MP residues has chaotic behavior, we conjecture that, for most signal sources, MP angles can be approximately modeled as statistically independent and identically distributed (iid) after the first MP iteration. In Section 4.2, we state a result, which is later proved in Appendix A, regarding dictionaries that include an orthonormal basis. For such dictionaries, after a number of iterations greater than or equal to the signal space dimension, the MP has a non-zero probability of obtaining an exact signal representation. From this result, one may adopt for such dictionaries two sets of statistics. One is used whenever the iteration number is smaller than the dimension of the signal space and another in the remaining cases, i.e., when the iteration number is greater than or equal to the signal space dimension. Considering the approximate statistical model of MP coefficients as being iid it is possible to obtain Lloyd–Max quantizers for MP coefficients independently of the signal source considered, as presented in Section 5. The Lloyd–Max quantizer (LMQ) presented is compared to the state-of-the-art off-loop MP quantization [18] in Section 6. Results show that both quantization schemes have similar rate-$\times$ distortion (RD) performance corroborating that the iid statistical model for MP angles is appropriate to be used in practice. Section 7 concludes the paper.

2. Off-loop quantization of MP coefficients

Let the dictionary be $\mathcal{D}=\{\mathbf{g}_k\}$ and $k\in\{1,\ldots,\#_{\mathcal{D}}\}$ such that $\|\mathbf{g}_k\|=1\ \forall k$, where $\#_{\mathcal{D}}$ is the dictionary cardinality, i.e., the number of elements in $\mathcal{D}$. In each iteration $m\geq 1$, the MP searches for the atom $\mathbf{g}_{i(m)}\in\mathcal{D}$, i.e., $i(m)\in\{1\ldots\#_{\mathcal{D}}\}$, with largest inner product with the residual signal $\mathbf{r}_{\mathbf{x}}^{m-1}$ [1,2]. The initial residue is $\mathbf{r}_{\mathbf{x}}^{0}=\mathbf{x}$. The residue of each iteration is given by $\mathbf{r}_{\mathbf{x}}^{m}=\mathbf{r}_{\mathbf{x}}^{m-1}-\gamma_m\mathbf{g}_{i(m)}$, where $\gamma_m=\langle\mathbf{r}_{\mathbf{x}}^{m-1},\mathbf{g}_{i(m)}\rangle$ is the inner product between $\mathbf{r}_{\mathbf{x}}^{m-1}$ and the atom $\mathbf{g}_{i(m)}$. The atom and the residue resulting of each MP iteration are orthogonal. Therefore, one can express $\mathbf{x}$ using the M-term representation (or simply M-term)

$$\hat{\mathbf{x}}\approx\sum_{m=1}^{M}\gamma_m\mathbf{g}_{i(m)}, \tag{1}$$

where $\mathbf{g}_{i(m)}$ is the atom selected at the m-th MP iteration and γ_m is referred to as the m-th MP coefficient. After M MP iterations, the approximation error is the M-th residue $\mathbf{r}_{\mathbf{x}}^{M}=\mathbf{x}-\hat{\mathbf{x}}$. Note that the MP is non-linear, since the decomposition of $\mathbf{x}=\mathbf{x}_1+\mathbf{x}_2$ is not, in general, the sum of the decompositions of $\mathbf{x}_1$ and $\mathbf{x}_2$. In practice, the MP (the calculation of γ_m, $i(m)$, and $\mathbf{r}_{\mathbf{x}}^{m}$) is iterated until: (a) a prescribed distortion ($\|\mathbf{r}_{\mathbf{x}}^{m}\|$) is met, (b) a maximum number of steps M is achieved, or, (c) either a small decay rate or a stationary behavior for the approximation metric ($|\gamma_m|/\|\mathbf{r}_{\mathbf{x}}^{m-1}\|$) is observed [2,4,5].

A common practice for compressing MP decompositions is to quantize the coefficients off-loop. In this scheme, first the decomposition is obtained and then its coefficients are quantized. That is, the quantizer is placed outside the decomposition loop with the residues being computed without considering the quantization. In these cases the quantization may be either applied off-line, that is, after the entire M-term is available such that all the M coefficients are provided to the coder, or on-line, i.e., each γ_m is quantized as soon as it is available. On-line coding delivers the quantized coefficients at an earlier stage than off-line, allowing the decomposition to be halted once the available rate is achieved. On the other hand, off-line coding allows for the conceptually simple rate $\times$ distortion (RD) optimization procedure consisting of trying different quantizers in order to find one meeting a prescribed RD criterion.

The state-of-the-art for off-loop quantization of MP coefficients is the adaptive exponentially upper bounded quantization (EUQ) [18]. It allocates bits and sets the quantizer dynamic range for each coefficient in the MP decomposition. It accomplishes this by first sorting all the coefficients in decreasing magnitude order, and subsequently employing a uniform quantizer of distinct dynamic range and number of levels for each coefficient. The quantizer range for the m-th coefficient depends on the quantized value of the $(m-1)$-th coefficient, and the

number of levels of each quantizer is decided using a bit-allocation scheme based on a Lagrangian multiplier [18,23]. In order to allow the decoder to perform the inverse quantization, the value of the largest coefficient and the number of bits used to quantize the second largest coefficient are sent as side information. This scheme has a good RD performance particularly at low bit-rates [18]. Note that we have chosen to benchmark the proposed statistical model of MP angles by designing a Lloyd–Max quantizer and comparing its performance to the one of the EUQ, which has good RD performance. If the results of the Lloyd–Max quantizer and the EUQ are comparable, we have an indication of the usefulness of the proposed statistical model.

When the M-term is quantized off-loop the signal is retrieved using

$$\hat{\mathbf{x}}_q = \sum_{m=1}^{M} Q[\gamma_m]\mathbf{g}_{i(m)}, \tag{2}$$

where $Q[\gamma_m]$ is the quantized value of coefficient γ_m. The quantization error relative to the actual signal is given by $\mathbf{d} = \mathbf{x} - \hat{\mathbf{x}}_q$ and leads to the energy distortion per sample

$$d^2 = \frac{1}{N}\|\mathbf{d}\|^2 = \frac{1}{N}\|\mathbf{x} - \hat{\mathbf{x}}_q\|^2, \tag{3}$$

where N is the signal dimension. However, since $\mathbf{x} = \hat{\mathbf{x}} + \mathbf{r}_{\mathbf{x}}^M$, then d^2 is influenced by the residual signal; therefore, d^2 does not depend only on the quantization of the coefficients. In order to consider just the distortion due to quantization, we employ the quantization error of the M-term

$$\mathbf{d}_M = \hat{\mathbf{x}} - \hat{\mathbf{x}}_q = \sum_{m=1}^{M} (\gamma_m - Q[\gamma_m])\mathbf{g}_{i(m)}, \quad d_M^2 = \frac{1}{N}\|\hat{\mathbf{x}} - \hat{\mathbf{x}}_q\|^2. \tag{4}$$

Noting that $\mathcal{D}$ is composed of unit norm vectors ($\|\mathbf{g}_k\| = 1,\ \forall k \in [1, \#_{\mathcal{D}}]$) and defining

$$e_q(\gamma_m) = \gamma_m - Q[\gamma_m], \tag{5}$$

the energy distortion per sample of the quantized M-term is given by

$$d_M^2 = \frac{1}{N}\left[\sum_{m=1}^{M} e_q^2(\gamma_m) + \sum_{m=1}^{M}\sum_{\substack{l=1 \\ l\neq m}}^{M} e_q(\gamma_m)e_q(\gamma_l)\langle \mathbf{g}_{i(m)}, \mathbf{g}_{i(l)}\rangle\right], \tag{6}$$

For a given signal source $\mathcal{X}$, one may consider the expected value of d_M^2

$$E[d_M^2] = \frac{1}{N}\left\{\sum_{m=1}^{M} E[e_q^2(\Gamma_m)] + \sum_{m=1}^{M}\sum_{\substack{l=1 \\ l\neq m}}^{M} E[e_q(\Gamma_m)e_q(\Gamma_l)\langle \mathbf{g}_{i(m)}, \mathbf{g}_{i(l)}\rangle]\right\}. \tag{7}$$

In this equation, Γ_m is a random variable (RV) corresponding to γ_m, for $1 \le m \le M$, for the signal source $\mathcal{X}$. One should note that no assumption has been imposed on the number of decomposition steps M, that is, Eq. (7) is valid for any M, small or large. For designing an efficient quantizer the statistics of Γ_m are required. However, the statistics of MP coefficients vary across iterations [18]. Instead of searching for a statistical model for MP coefficients, we employ a statistical model for the angles in MP iterations which is discussed below.

3. Angles in matching pursuit iterations

Let the dictionary be $\mathcal{D} = \{\mathbf{g}_k\}$, considering that $\|\mathbf{g}_k\| = 1$, $\forall k \in \{1, \ldots, \#_{\mathcal{D}}\}$, at the m-th MP iteration the angle between the residue $\mathbf{r}_{\mathbf{x}}^{m-1}$ and the selected atom $\mathbf{g}_{i(m)}$ is

$$\theta_m = \arccos\left(\frac{\langle \mathbf{r}_{\mathbf{x}}^{m-1}, \mathbf{g}_{i(m)}\rangle}{\|\mathbf{r}_{\mathbf{x}}^{m-1}\|}\right). \tag{8}$$

If $\mathbf{g}_k \in \mathcal{D}$ implies that $-\mathbf{g}_k \in \mathcal{D}$, then the γ_m are always positive. In the sequel we assume that the dictionaries possess this property. If this is not the case for a given dictionary $\mathcal{D}'$, then we create a new dictionary $\mathcal{D} = \mathcal{D}' \cup \mathcal{D}''$, where $\mathcal{D}'' = \{-\mathbf{g}_k\} \forall \mathbf{g}_k \in \mathcal{D}'$. This may require one more bit to index the atoms but since one saves the coefficient's sign bit, the data rate of the M-term is unaltered. With $\mathcal{D}$ having this property, we have that

$$\gamma_1 = \|\mathbf{x}\|\cos(\theta_1); \quad \|\mathbf{r}_{\mathbf{x}}^1\| = \|\mathbf{x}\|\sin(\theta_1) \tag{9}$$

$$\gamma_2 = \|\mathbf{x}\|\sin(\theta_1)\cos(\theta_2); \quad \|\mathbf{r}_{\mathbf{x}}^2\| = \|\mathbf{x}\|\sin(\theta_1)\sin(\theta_2) \tag{10}$$

$$\vdots \quad \vdots$$

$$\gamma_m = \|\mathbf{x}\|\left[\prod_{i=1}^{m-1}\sin(\theta_i)\right]\cos(\theta_m); \quad \|\mathbf{r}_{\mathbf{x}}^m\| = \|\mathbf{x}\|\prod_{i=1}^{m}\sin(\theta_i). \tag{11}$$

A relevant dictionary metric is the maximum angle between any signal $\mathbf{x}$ belonging to the signal space $\mathbb{X}$ and its closest atom in $\mathcal{D}$

$$\Theta(\mathcal{D}) = \arccos\left(\min_{\mathbf{x}\in\mathbb{X}}\left[\max_{i\in\{1,\ldots,\#_{\mathcal{D}}\}}\left(\frac{|\langle \mathbf{x}, \mathbf{g}_i\rangle|}{\|\mathbf{x}\|}\right)\right]\right). \tag{12}$$

This dictionary metric was used in [24] in the context of successive approximation vector quantization. In the context of matching pursuit algorithms, it has also been called structural redundancy [25].

Since $\theta_m \le \Theta(\mathcal{D})$ then Eq. (11) implies that the residue at the m-th step is bounded by

$$\|\mathbf{r}_{\mathbf{x}}^m\| \le \|\mathbf{x}\|\sin^m(\Theta(\mathcal{D})). \tag{13}$$

However, this bound is weak, since θ_i is in general distributed between zero and $\Theta(\mathcal{D})$. Note that Eq. (13) also leads to the known fact that MP expansions converge if $\mathcal{D}$ spans the signal space [2,4,26], since, in this case, $\Theta(\mathcal{D}) < \pi/2$.

Although Eq. (13) bounds the norm of MP residues and, therefore, the norm of MP coefficients, subsequent MP coefficients may not decrease in magnitude. Theorem 1 uses $\Theta(\mathcal{D})$ to find an upper bound for the number of MP iterations required such that the coefficient magnitude decreases.

Theorem 1. *After*

$$l = \left\lceil \frac{\log[\cos(\Theta(\mathcal{D}))]}{\log[\sin(\Theta(\mathcal{D}))]} \right\rceil \text{ steps}, \tag{14}$$

the MP always produces coefficients $\gamma_{m+l} \le \gamma_m$.

Proof. Since $\gamma_m = \|\mathbf{x}\|[\prod_{i=1}^{m-1}\sin(\theta_i)]\cos(\theta_m)$ and $\gamma_{m+l} = \|\mathbf{x}\|[\prod_{i=1}^{m+l-1}\sin(\theta_i)]\cos(\theta_{m+l})$ it follows that

$$\gamma_{m+l} = \gamma_m \tan(\theta_m)\sin(\theta_{m+1})\ldots\sin(\theta_{m+l-1})\cos(\theta_{m+l}).$$

Given γ_m the largest possible value of γ_{m+l} is obtained if $\theta_i = \Theta(\mathcal{D})\ \forall i \in [m,\ldots,m+l-1]$ and $\theta_{m+l} = 0$. Thus, one can guarantee that $\gamma_{m+l} \le \gamma_m \tan(\Theta(\mathcal{D}))[\sin(\Theta(\mathcal{D}))]^{l-1}$. Therefore, if $\tan(\Theta(\mathcal{D}))[\sin(\Theta(\mathcal{D}))]^{l-1} \le 1$ then $\gamma_{m+l} \le \gamma_m$, what is equivalent to

$$l \ge \frac{\log[\cos(\Theta(\mathcal{D}))]}{\log[\sin(\Theta(\mathcal{D}))]}, \tag{15}$$

which implies Eq. (14). □

Theorem 1 shows that once $\Theta(\mathcal{D})$ is known, the number of iterations l guaranteeing that the coefficient magnitude decreases is also known. Note that the bound provided by Theorem 1 is weak for the same reasons that the bound in Eq. (13) is weak. In addition, it is a difficult task to obtain $\Theta(\mathcal{D})$ for a given $\mathcal{D}$ and, in practice, statistical estimates may suffice and can be obtained by decomposing a large set of signals from a randomly generated uniformly oriented source [27].

4. Statistics of the angles in MP iterations

Consider a memoryless independent and identically distributed (iid) N-dimensional Gaussian source $\mathcal{N}(0,\sigma^2)$. It is a well known fact that its pdf depends just on the vector magnitude [28]. Therefore, if one normalizes the outcomes $\mathbf{x}$ such that $\|\mathbf{x}\| = 1$, then the resulting source will be uniform on the unit sphere. Fig. 1 illustrates this fact by presenting the probability density functions (pdf) of the orientation of normalized vectors that are drawn from four different two dimensional random sources. The figure shows that the orientation of the Gaussian source is uniformly distributed.

It has been observed that after the first iterations, MP residues have a chaotic behavior [29]. Thus it is reasonable to assume that, after some MP iterations, MP residues do not have any preferred orientation in the signal space, or, in more precise terms that their probability distribution depends just on their magnitude. Thus, one could assume that, if one normalizes the residuals such that $\|\mathbf{r}_{\mathbf{x}}^{i}\| = 1$ then, after the first MP step, they have a pdf that is uniform on the unit sphere. Since this is the same property enjoyed by the normalized iid Gaussian source, it seems reasonable to assume that a normalized iid Gaussian source may be a good model to such normalized MP residues. If this assumption is true then one may expect that after their first iterations, the angles between the selected atoms and the MP residues may have a similar distribution to the one obtained for the angle in the first MP iteration for a memoryless iid Gaussian source.

We now investigate the validity of the above argument. In order to do so, we start by using dictionaries $\mathcal{D}$ composed by normalized outcomes of a Gaussian iid source. Such dictionaries composed by outcomes of random processes have been often used [3,18] to investigate properties of decomposition algorithms. We refer to a dictionary composed of $\#_{\mathcal{D}}$ unit-norm signals obtained by normalizing outcomes of an N-dimensional Gaussian source as $GSND(\#_{\mathcal{D}},N)$. Fig. 2 shows the pdfs (actually, histograms normalized to have unit area) of the RVs (random variables) Θ_m, which correspond to the angles in the m-th MP iteration (for several m). These pdfs result from decompositions of realizations of a memoryless iid Gaussian source using a $GSND(16,4)$. Fig. 3 shows the mean and the variance of Θ_m for several m together with the covariance among some Θ_m for the same dictionary and source. The results in Figs. 2 and 3 were obtained using an ensemble of 50,000 MP decompositions of signals from the Gaussian source. In Fig. 2 it can be verified that the pdfs of the RVs Θ_m have a similar shape for all m. This corroborates the above assumptions about the MP residue's pdf, leading to the conjecture that the pdfs $f_{\Theta_m}(\theta_m)$ are independent of the MP iteration number m and identically distributed across MP iterations. Note that this conjecture is consistent with the results presented in [29,4], where it is shown that, under specific conditions, the MP has a chaotic behavior, i.e., the residue in step m maps, chaotically, to the residue in step $m+1$.

Since in the example of Fig. 2 the angles Θ_m are approximately identically distributed, one argues whether

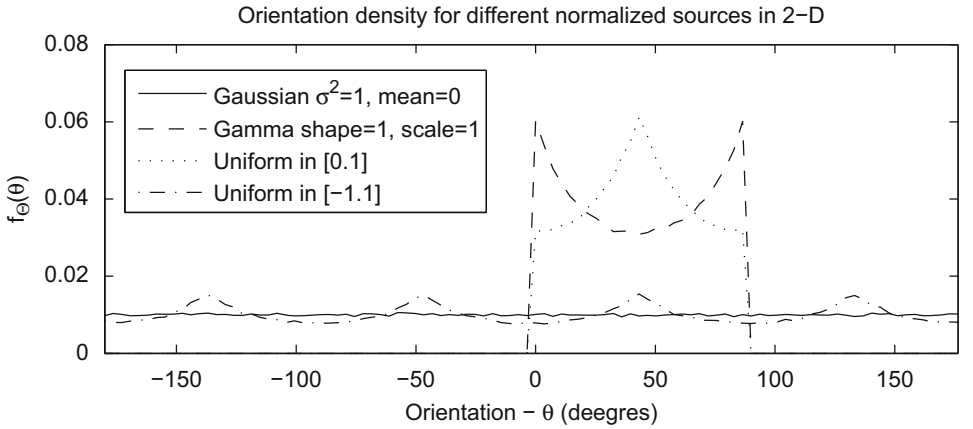

Fig. 1. Probability density functions of the orientation of normalized vectors drawn from different random sources in $\mathbb{R}^2$.

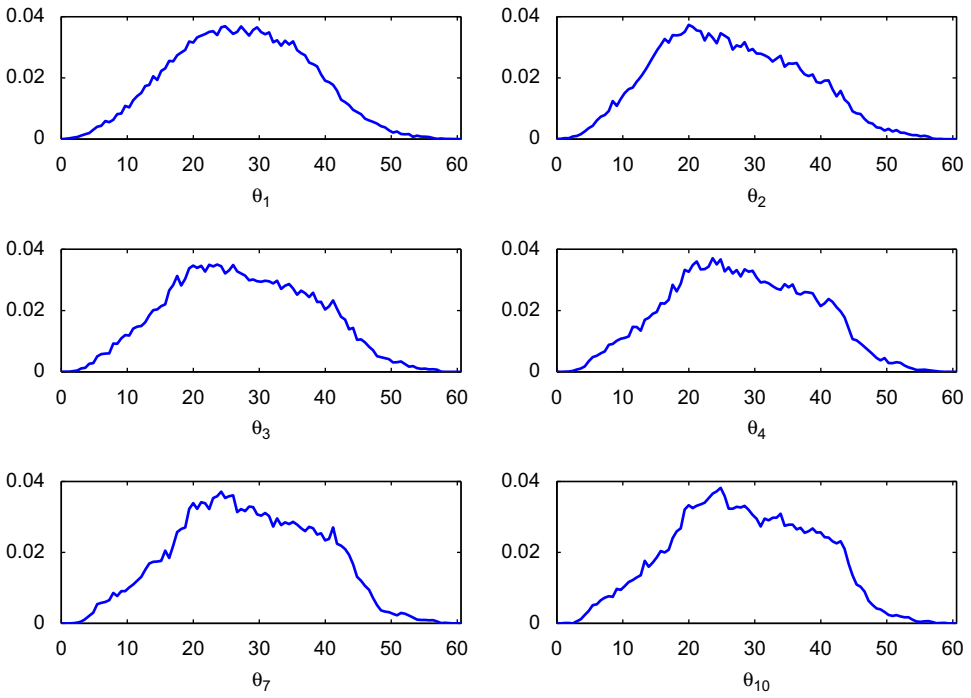

Fig. 2. Probability density functions of Θ_m for a Gaussian source of $\mathbb{R}^4$ using the *GSND*(16,4).

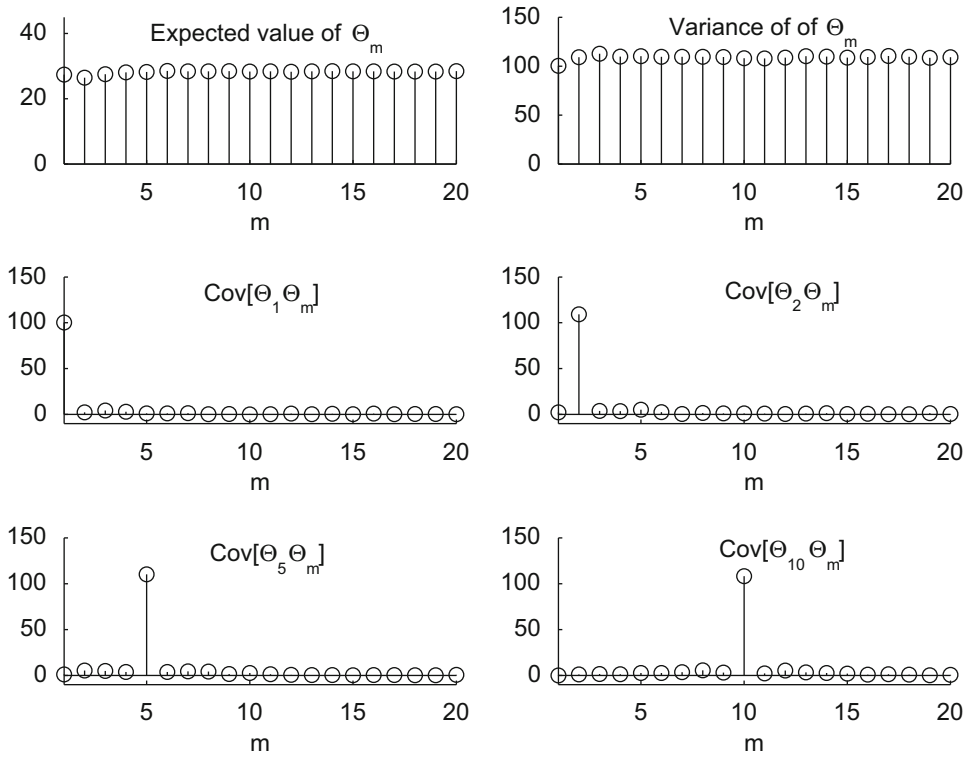

Fig. 3. Mean, variance and covariance of Θ_m for a Gaussian source in $\mathbb{R}^4$ using the *GSND*(16,4).

they can be also modeled as statistically independent. Fig. 3 gives us a hint on that. It depicts the covariances between MP angles in different steps. As can be observed $\mathrm{Cov}[\Theta_i,\Theta_k] \approx c\delta(i-k)$ (c is a constant), i.e., the angles are uncorrelated. Of course, this does not imply the independence of the angles RVs, instead, it shows that the

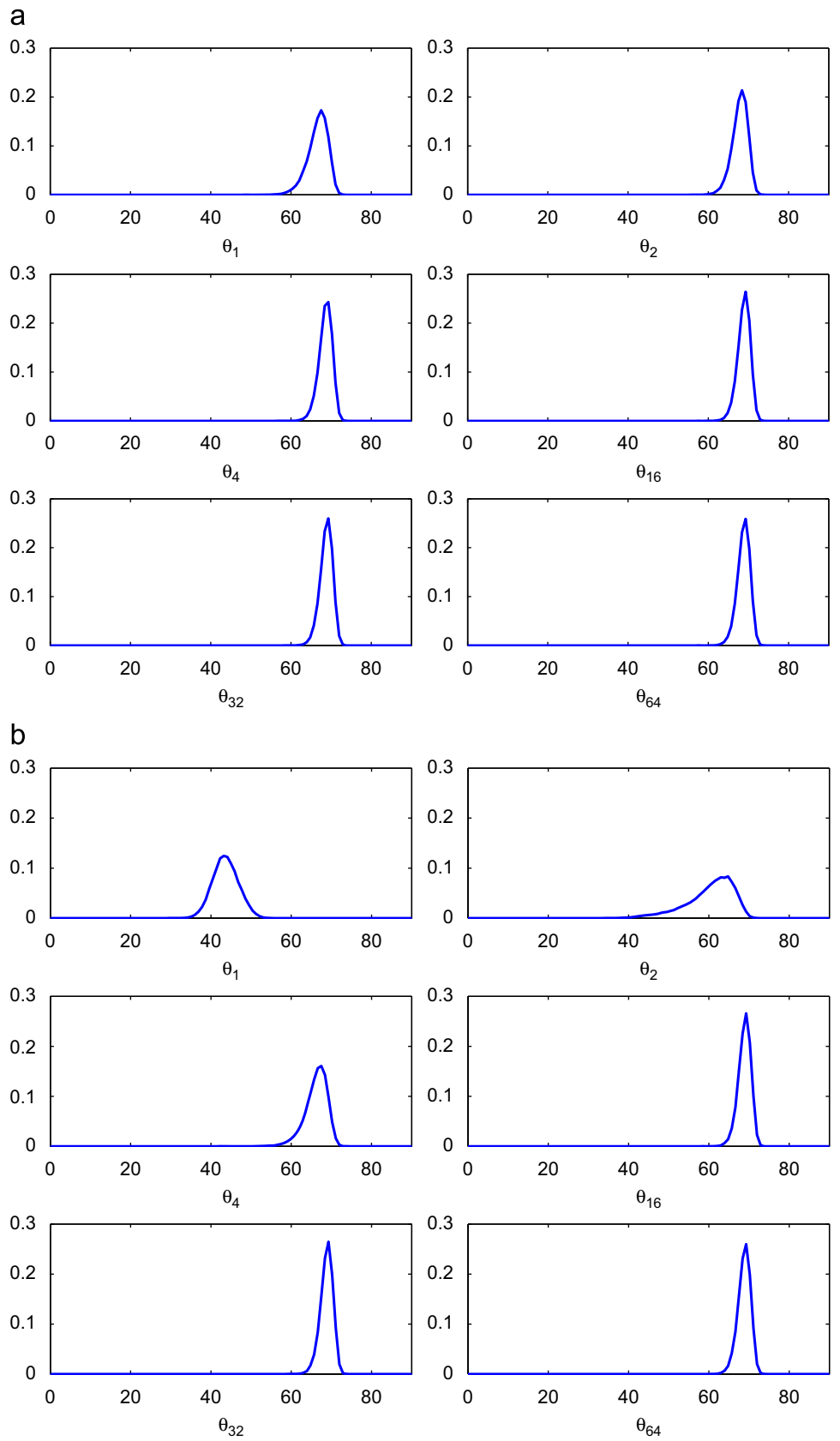

Fig. 4. Probability density functions of MP angles for two iid sources in $\mathbb{R}^{64}$ at iterations $m=\{1,2,4,8,16,32,64\}$, for the four-phase Gabor dictionary in $\mathbb{R}^{64}$. (a) Gaussian; (b) Gamma.

independence assumption is consistent with the observed covariance data. This suggests that it may be reasonable to model the angle RVs Θ_m as being statistically independent.

4.1. Angle statistics for the Gabor dictionary in $\mathbb{R}^{64}$

The results presented so far were obtained using a dictionary of relatively low dimension and cardinality. In practice the MP is commonly used in high dimensional spaces using parameterized dictionaries, as for example, the Gabor one [1,2]. The elements of the Gabor dictionary are defined by translations, modulations and dilations of a prototype signal [1,2,30]. The most common choice for the prototype signal $\mathbf{f}[n]$ is the Gaussian window. The atoms of the Gabor dictionaries are complex valued, as such, for obtaining real coefficients, the optimal phase for the atom can be computed [31,5]. However, in compression applications, a quantized phase is often employed. Therefore, we analyze here a real Gabor dictionary composed of atoms with phases being multiples of π/V, $V \in \mathbb{N}^*$. Each atom is then given by

$$g[n] = \begin{cases} \delta[n] & \text{if } j = 0 \\ K_{(j,p,k,\nu)} f\left[\dfrac{n-p2^j}{2^j}\right] \cos\left[nk\pi 2^{1-j} + \dfrac{\pi\nu}{V}\right] & \text{if } j \in (0, L) \\ \dfrac{1}{\sqrt{N}} & \text{if } j = L \end{cases}, \tag{16}$$

where $f[n] = 2^{1/4} e^{-\pi n^2}$, n is the coordinate, $K_{(j,p,k,\nu)}$ provides a unit-norm atom, and $\nu \in [0, \ldots, V-1]$. For the Gabor atom j defines its scale, p defines the time shift, and k defines the atom modulation. For $L = \log_2(N)$ scales, the atom parameters ranges are $j \in [0,L]$, $p \in [0, N2^{-j})$, $k \in [0, 2^j)$, and $\nu \in [0, V-1]$.

Fig. 4(a) shows $f_{\Theta_m}(\theta_m)$, the pdfs of the RVs Θ_m, for some m, obtained for an ensemble of 512,000 decompositions of signals from the $\mathbb{R}^{64}$ Gaussian source using a four-phase Gabor dictionary (V=4). Fig. 4(b) shows $f_{\Theta_m}(\theta_m)$, for some m, obtained for an ensemble of 512,000 decompositions of signals driven from a memoryless source that has Gamma distributed coordinates in $\mathbb{R}^{64}$ for the same dictionary. Note that the statistics of the angles from these two sources differ significantly at the first MP iteration, but become closer as the iteration number m increases. The results in Fig. 4 show that, for an iteration number between 4 and 16, MP angles start to have very similar statistics for both the Gaussian and the Gamma source. In addition, for both sources the statistics of these angles are very similar to the ones that are obtained in the first iteration for a Gaussian source. Indeed, for any source, as m increases the pdfs of the angles in different MP steps get more similar to the ones obtained for a Gaussian source. Similar results were observed for decompositions of signals taken from a source uniformly distributed in the unit-length cube and also for 8×8 image blocks taken from frontal x-ray images. The pdf of the angles across different iterations when decomposing those image blocks with the same dictionary are shown in Fig. 5.

One should note that, although the statistics for other sources are not exactly equal to the statistics obtained for the first decomposition stage of signals from the Gaussian source, they are reasonably close to the later. Therefore, the pdf of the first MP angle, $f_{\Theta_1}(\theta_1)$, obtained for a memoryless iid Gaussian source, may be an acceptable model for $f_{\Theta_m}(\theta_m)$, $m > 1$, for any signal source. This further corroborates the assumption made above that, after the first step, the MP residuals when normalized to unit-energy are uniformly

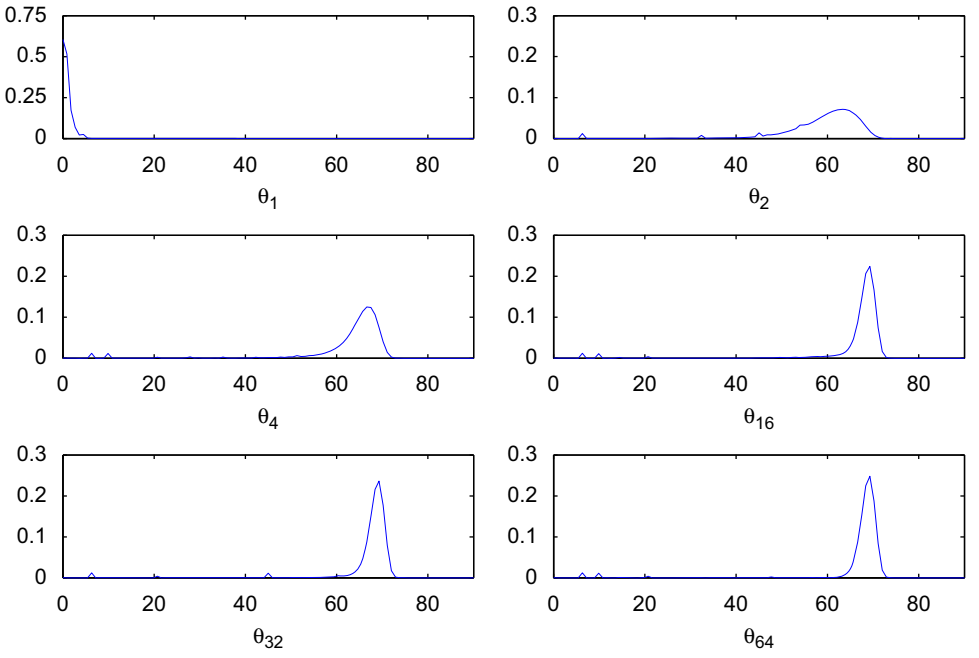

Fig. 5. Probability density functions of MP angles when decomposing 8×8 blocks taken from s-ray images at iterations m={1,2,4,8,16,32,64}, for the four-phase Gabor dictionary in $\mathbb{R}^{64}$.

distributed over the unit sphere. Fig. 6 presents the mean and the variance of the MP angles as well as the covariance between the angles in MP iterations for the decomposition of the same Gaussian source ensemble. As can be observed, similarly to the case for *GSND*(16,4) (see Fig. 3), the covariance between Θ_m and Θ_{m+l} quickly decreases with l. This indicates that, even when the dimensionality of the signal space is high, to model the Θ_m as independent may be a reasonable and accurate assumption.

4.2. Dictionaries including orthonormal bases

In the particular case that the dictionary includes an orthonormal basis, the assumption that the MP residues after the first step are identically distributed has to be slightly reformulated. This is so because, as we demonstrate here, for such a dictionary, under very general conditions, the MP algorithm has a non-zero probability of generating null residues in a finite number of steps. We refer to it as the null residue proposition. In essence it shows that there exists a region of the space, of volume greater than 0, such that all vectors belonging to it lead to a null residue after a finite number of MP iterations. Its proof is presented in Appendix A, where it is shown that if $\mathcal{D}$ includes an orthonormal basis then the MP has a non-zero probability of trapping the residuals of the MP decomposition of a given vector into successive subspaces that are orthogonal to the previously selected atoms. Therefore, since at any iteration m it is known that the residual $\mathbf{r}_{\mathbf{x}}^m$ is orthogonal to $\mathbf{g}_{i(k)}$, $k=1,2,\ldots m$, then there is a non-zero probability that the MP will produce a null residue ($\mathbf{r}_{\mathbf{x}}^q = \vec{0}$) in a finite number of steps $q \geq N$. Details on the conditions necessary for this to hold can also be found in Appendix A.

For example, when a *GSND*(20,4) is used to decompose an ensemble of 25,600 signals drawn from a four

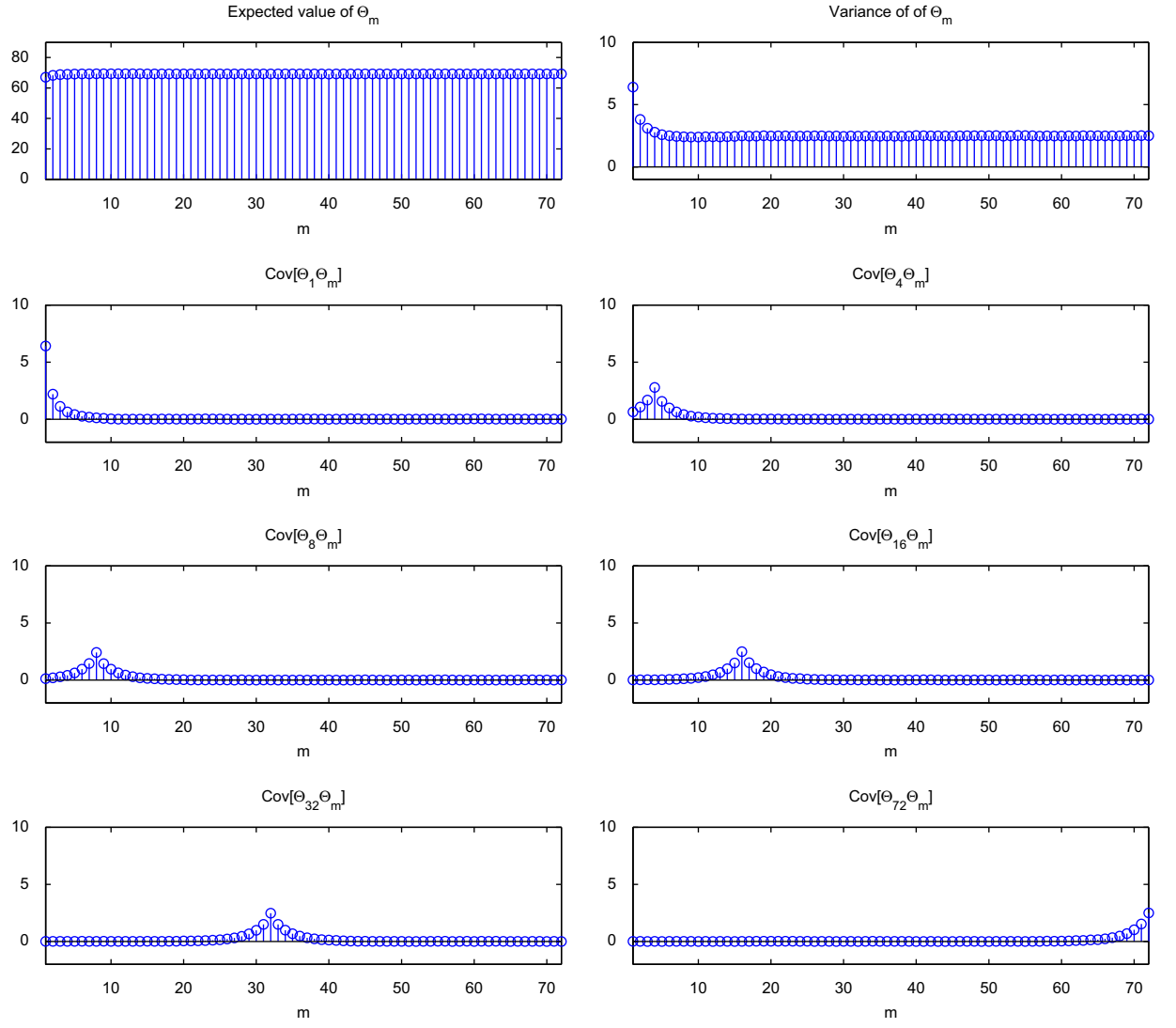

Fig. 6. Mean, variance and covariance between angles in MP iterations for a Gaussian source in $\mathbb{R}^{64}$ as a function of the iteration for the Gabor dictionary in $\mathbb{R}^{64}$ of four phases.

dimensional memoryless Gaussian source, allowing at most 100 decomposition steps, none of the signal decompositions produces a null residue. However, once a set of four elements of the same *GSND*(20,4) is replaced by the canonical basis of $\mathbb{R}^4$, exact signal expansions with finite number of terms are obtained. Fig. 7 shows the histogram of the number of null residues produced by the MP as a function of the MP iteration for an ensemble of 25,600 signals drawn from a four dimensional memoryless Gaussian source when the *GSND*(20,4) is modified to include the canonical basis of $\mathbb{R}^4$. The last bin of the histogram accounts for the decompositions that did not produce null residues. From this figure one can see that there are indeed signals that are decomposed with a null residue for a number of iterations greater than or equal to 4 (the signal dimension). This is in accordance with the results in Appendix A, where Corollary 1 shows that for an iid Gaussian source the MP has a non-zero probability of producing null residues after N (the signal space dimension) iterations.

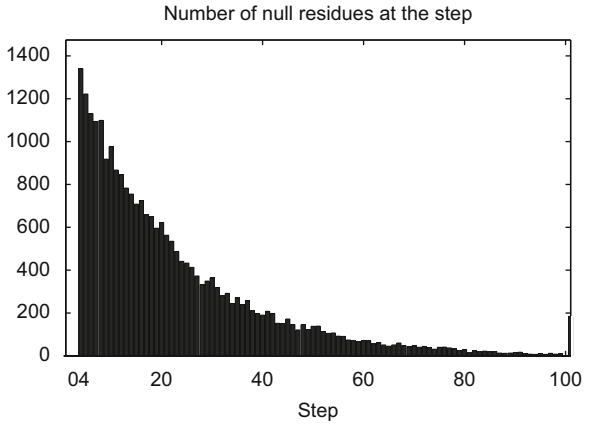

Fig. 7. Incidence of null residues using a *GSND*(20,4) with four elements replaced by the canonical basis of $\mathbb{R}^4$.

The null residue proposition is further illustrated in Fig. 8, that shows the pdfs of the angles at steps 1, 4 and 8 for the aforementioned decomposition process. On the left-hand side of Fig. 8 are shown results for the original *GSND*(20,4) dictionary, and on the right-hand side for the modified *GSND*(20,4) dictionary. One observes on the left-hand side of Fig. 8 that for the original *GSND*(20,4) null angles do not occur, which is equivalent to saying that the MP decompositions never generate a null residue. On the other hand, the impulses that appear at $\Theta_i = 0$ ($i \in \{4,8\}$) on the right-hand side of Fig. 8 show that for the modified *GSND*(20,4) null angles often occur when $m \geq 4$. One should also note that for the modified *GSND*(20,4) the percentage of null angles are very similar after the fourth MP iteration. The probability of producing a null residue at a given MP step depends on both the dictionary $\mathcal{D}$ and on the signal source, and there is not yet a way to compute it theoretically; however, it can be estimated by simulation. For instance, in the example of Fig. 7, one can deduce from the presented data that the probability of having a null residue at step 4 is approximately 0.063.

A useful kind of such dictionaries are the ones including several distinct orthonormal bases. Among

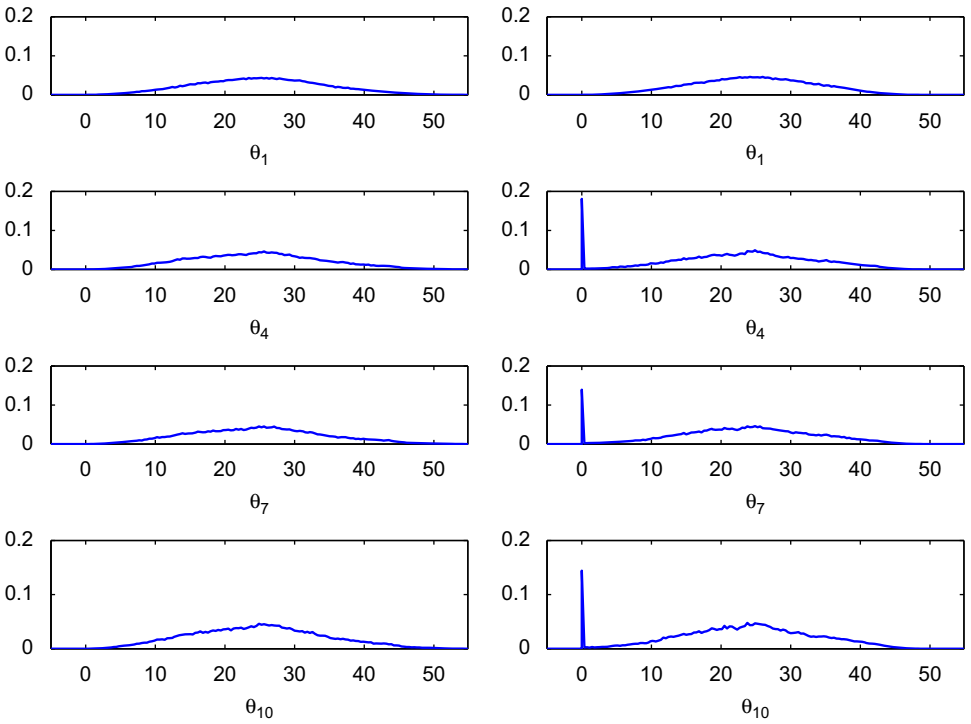

Fig. 8. Probability density functions of the angles at $m=\{1,4,8\}$ using the original *GSND*(20,4) (left) and the modified *GSND*(20,4) (right)—the *GSND*(20,4) with four of its elements replaced by the canonical basis of $\mathbb{R}^4$.

them one can highlight the dictionaries that are unions of orthonormal bases [2,32,6]. An example of a dictionary composed by a union of bases is the dictionary formed by the normalized elements of the first shell of the ε_8 lattice [33,34] (the ε_{8,sh_1} dictionary). It is composed by 240 elements (in 120 directions) in $\mathbb{R}^8$, and for each of its elements it contains either 126 or 110 orthogonal elements. Actually, the ε_{8,sh_1} dictionary can be regarded as the union of 30 bases for $\mathbb{R}^8$. Fig. 9 shows the pdfs of the MP angles Θ_m, $m \in \{1,\ldots,10\}$, for ε_{8,sh_1}. They were obtained using an ensemble of 512,000 MP decompositions of Gaussian source signals. In Fig. 9, it is possible to verify that the pdfs of $\Theta_m, m \in \{1,\ldots,7\}$ are reasonably similar. Note also that, after a number of steps m greater than or equal to 8 (the space dimension) the pdfs of the different Θ_m are also quite similar and have a large incidence of zero angles. The above results show that, when the $\varepsilon_{8,sh1}$ dictionary is employed, the statistics of the first MP angle for a memoryless white Gaussian source are appropriate to model the angles in the first seven decomposition steps. However, after the eighth step, they are not appropriate anymore. Nevertheless, the results imply that only two distinct pdfs are needed to model the MP angles for the $\varepsilon_{8,sh1}$: one pdf being valid up to the seventh step and another being valid for step 8 and beyond.

In order to better understand how the probability of producing null residues varies with the space dimension, we generated dictionaries with a fixed ratio of the number of bits necessary to represent an element of the dictionary to the number of bits needed to encode an element of a basis, that is, $\log_2 \#_{\mathcal{D}} / \log_2 N = 1+\alpha$ (α can be regarded as a redundancy factor). In this case the dictionary cardinality would be $\lceil N^{1+\alpha} \rceil$. Fig. 10 shows the probability of convergence for a $GSND(\lceil N^{1+\alpha} \rceil, N)$ for $\alpha = 0.25$ and $N \in [1,\ldots,53]$ with N of its elements replaced by the canonical basis. One observes that the probability of convergence has an approximately exponential decrease with N.

4.3. Discussion

In [29,4], the average value of the approximation ratio $|\gamma_m| / \|\mathbf{r}_{\mathbf{x}}^{m-1}\|$ was studied. It corresponds to the cosine of the angle between the MP residual and the atom at the m-th step. In those works it is discussed that the mean of the approximation ratio converges to a fixed value. Here we support a stronger claim. We have observed that, after the first iterations, the statistics of the angles between residuals and atoms can be considered to be almost invariant across iterations. This happens for sources with

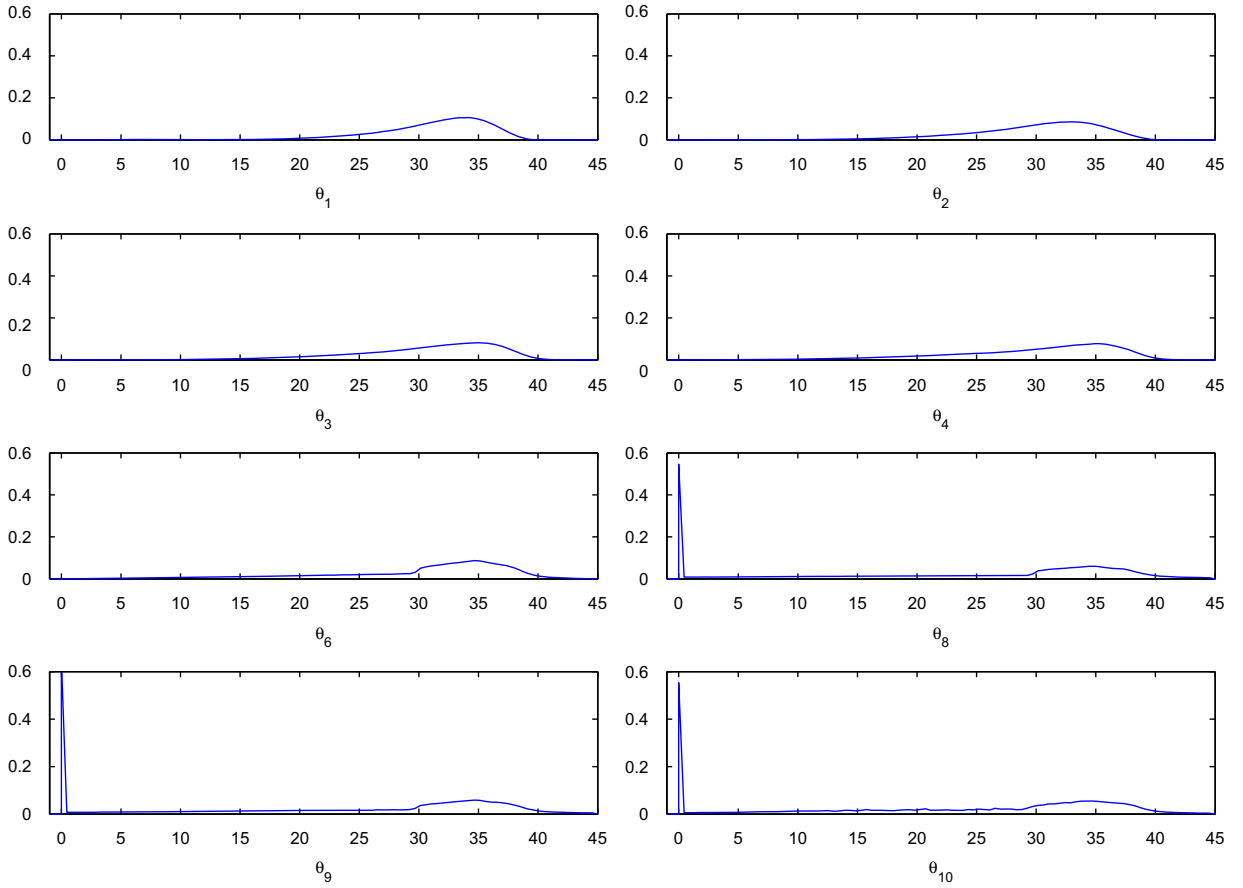

Fig. 9. Probability density functions of Θ_m for a Gaussian source in $\mathbb{R}^8$ using the ε_{8,sh_1} dictionary.

very different angle statistics, as is the case for the Gamma and Gaussian sources and x-ray image blocks (refer to Figs. 1, 4, and 5). Exceptions occur when the dictionary includes an orthonormal basis; since in these cases two different pdfs have to be used to model the angles in MP iterations, one valid at step numbers that are smaller than the signal dimension and another for the remaining steps—the ones that are greater than or equal to the signal space dimension.

The analysis of Fig. 4 shows that, for the Gabor dictionary the pdf of the angle between residuals and atoms, after some MP iterations, is reasonably similar to the pdf obtained in the first MP iteration of the decomposition of a memoryless Gaussian source. This indicates that one might use a Gaussian source to obtain good estimates of the pdf of the angle in MP iterations.

For measuring the quality of these estimates some metric is necessary. For evaluating the statistical similarities of the angles in MP iterations for different sources we use an "information similarity" metric, the Kullback–Leibler divergence [35]. For discrete sources it is defined as

$$D_{KL}(P||Q) = \sum \Pr(P(i)) \log_2 \frac{\Pr(P(i))}{\Pr(Q(i))}. \tag{17}$$

The Kullback–Leibler divergence can be interpreted as a measure of the extra bits that would be required for coding outcomes of a source P using an optimal code designed for the source Q. The larger the $D_{K,L}$ between two distributions the more different the distributions are. It is capable of capturing statistical differences between two sources from a "quantity of information" point of view. It can vary from zero (identical distributions) to infinity.

Fig. 11 shows D_{KL} between the distributions of the angles in different decompositions steps for the four-phases Gabor dictionary in $\mathbb{R}^{64}$. These were computed using histograms of 200 bins for the angles. Since $D_{KL}(P,Q) \neq D_{KL}(Q,P)$, we show the divergences computed in "both directions", i.e., interchanging the distributions roles in Eq. (17). Fig. 11(a) shows the D_{KL} between the distributions of the angles in different decomposition steps for a Gaussian source, while Fig. 11(b) shows the results for the Gamma source. One can observe that the divergences between the angle in the first decomposition step and subsequent ones for the Gaussian source are much smaller than for the Gamma source. For the Gaussian source, this suggests that it is reasonable to approximate the angle distribution $f_{\Theta_m}(\theta_m)$ for $m \neq 1$ using $f_{\Theta_1}(\theta_1)$. That is, the distribution of the angles in the first

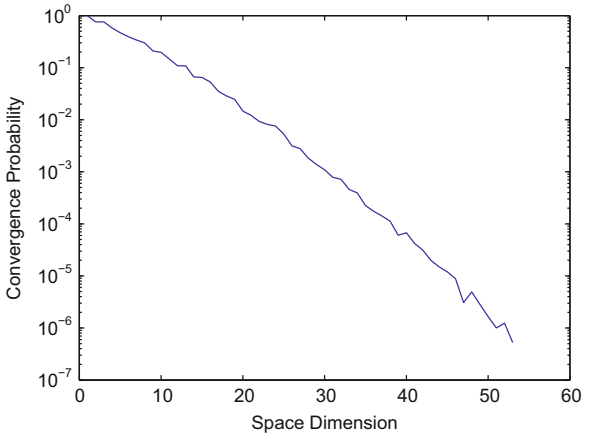

Fig. 10. Probability of convergence for a $GSND(\lceil N^{1+\alpha} \rceil, N)$ with N of its elements replaced by the canonical basis for $\alpha = 0.25$ and $N \in [1, \ldots, 53]$.

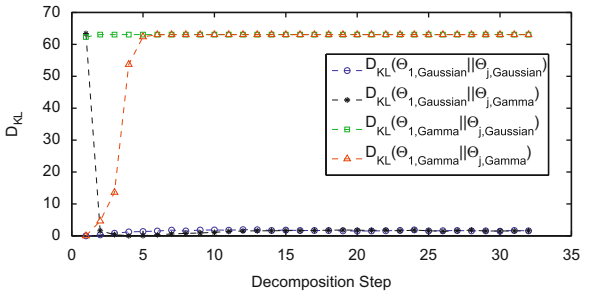

Fig. 12. Kullback–Leibler divergences between the first angle distribution and subsequent angles across Gaussian and Gamma sources for the four-phases Gabor Dictionary in $\mathbb{R}^{64}$.

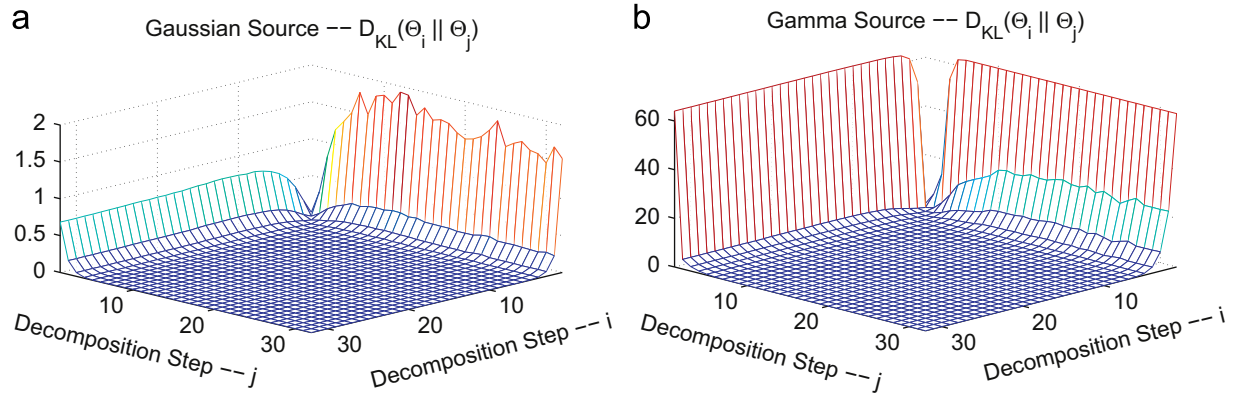

Fig. 11. Kullback–Leibler divergences between the angles in different decompositions steps for the four-phases Gabor Dictionary in $\mathbb{R}^{64}$. (a) Gaussian Source; (b) Gamma Source.

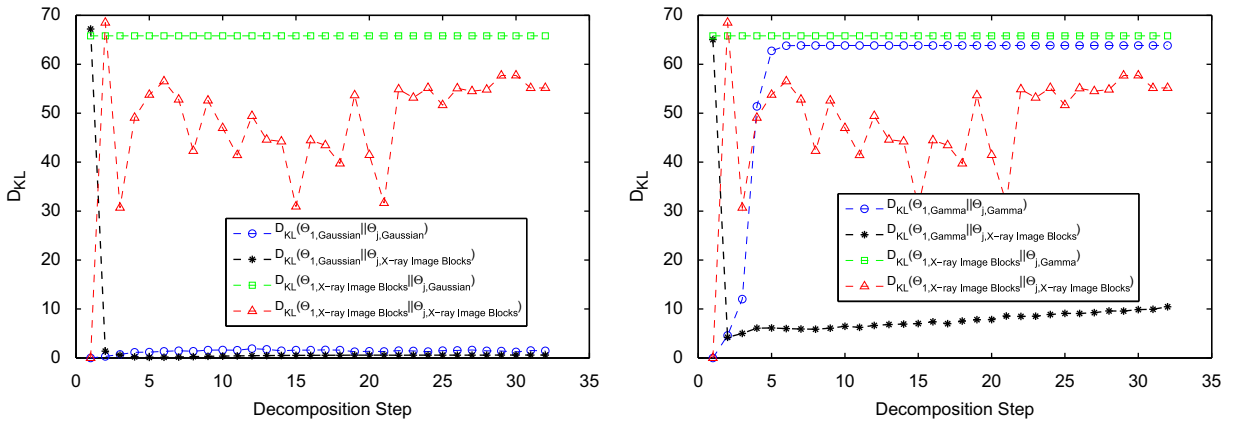

Fig. 13. Kullback–Leibler divergences between the first angle distribution and subsequent angles across Gaussian source and the source generated from 8×8 blocks from x-ray images for the four-phases Gabor Dictionary in $\mathbb{R}^{64}$, at the left; and across a Gamma distributed source and the x-ray image blocks source.

decomposition step of a Gaussian source captures reasonably well the distributions of the angles in following steps, what does not occur for the Gamma source.

Fig. 12 shows the Kullback–Leibler divergences between the angle distributions obtained for the first decomposition step of the Gaussian and Gamma sources and the ones obtained in subsequent steps for the two sources. One can see that the distribution of the angle in the first decomposition step of a Gaussian source is reasonably close to the ones obtained for both the Gaussian and the Gamma source after the first step. Fig. 13 presents in the left graph the results of the same experiment but between the Gaussian source and the source of x-ray 8×8 image blocks, where the same behavior can be observed. It also presents in the right graph the behavior of the Kullback–Leibler divergence across the Gamma and the x-ray image blocks source, in which case a different behavior is observed—none of the statistical models of the angle in the first MP iteration fits reasonably well the statistics of the angles in further MP iterations for those sources. However, as can be see, the Gaussian source is capable of obtaining such a model. Therefore, the results indicate that one could use a Gaussian source to obtain good estimates of the pdf of the angle in MP iterations after the first iteration, irrespective of the source distribution. As a result, the iid statistical model proposed in this section is an appropriate assumption.

In the sequel, we assess the effectiveness of this model by using it to design Lloyd–Max quantizers of MP coefficients. It should be noted that the statistics of the first MP angle, and therefore of the first coefficient, have a much higher degree of source dependence than in other MP steps, as confirmed by the results in Fig. 11. Therefore, in order, to make an appropriate use of the presented model for the angles between residuals and atoms, the first coefficient, γ_1, will be quantized with negligible error and encoded as side information. For coding the remaining coefficients a Lloyd–Max quantizer is designed considering that the statistics of the MP angles are invariant with respect to the iteration number and source. One should highlight that there is no goal of obtaining the best MP quantization ever, but to assess the usefulness of the proposed model of the pdf of MP coefficients by designing a Lloyd–Max quantizer using it.

5. Angle based Lloyd–Max quantizers for MP coefficients

In Eq. (11) the value of $\|\mathbf{x}\|$ is required to compute the coefficients. Alternatively, one can express the coefficients as a function of the first coefficient (γ_1), in this case Eq. (11) becomes

$$\gamma_m = \gamma_1 \delta_m, \quad \delta_m = \tan(\theta_1)\left[\prod_{i=2}^{m-1}\sin(\theta_i)\right]\cos(\theta_m), \quad m \geq 2. \tag{18}$$

Thus, the pdfs of the coefficients γ_m can be computed from the pdfs of the angles θ_m. For a known γ_1, the pdf of the RV Γ_m, for $m \geq 2$, is given by $f_{\Gamma_m}(\gamma_m|\gamma_1) = f_{\Gamma_m}(\gamma_1\delta_m|\gamma_1) = f_{\Delta_m}(\delta_m|\gamma_1)$, where Δ_m is the RV whose outcome is δ_m (defined in Eq. (18)). If an optimal quantizer $Q[\cdot]$ is designed for the RV Y, then the optimal quantizer for $Z=cY$ (c is a constant) is simply a scaled version of $Q[\cdot]$. Therefore, considering that instead of quantizing γ_m one quantizes δ_m (see Eq. (18)) and also that γ_1 is known, Eq. (7) becomes

$$E[d_M^2|\gamma_1] = \frac{\gamma_1^2}{N}\left\{\sum_{m=2}^{M} E[e_q^2(\Delta_m)] + \sum_{m=2}^{M}\sum_{\substack{l=2 \\ l\neq m}}^{M} E[e_q(\Delta_m)e_q(\Delta_l)\langle \mathbf{g}_{i(m)}, \mathbf{g}_{i(l)}\rangle]\right\}. \tag{19}$$

Thus, assuming γ_1 to be known, if the pdfs of the RVs Δ_m are known then $E[d_M^2|\gamma_1]$ can be computed for any $Q[\cdot]$ applied to Δ_m. For a given γ_1 the quantization of MP coefficients should aim to minimize the distortion per sample of the quantized M-term, defined in Eq. (19), incurring in the design of quantizers for Δ_m, $m \geq 2$. Since the quantization is applied to δ_m instead of γ_m, the value of γ_1 is required at the decoder and therefore has to be transmitted as side information. This strategy does not imply any extra bit-rate

cost; since when using the MP algorithm one has to transmit $\|\mathbf{x}\|$ as side information if one wants to use coefficient quantizers that are independent of the signal's dynamic range. If one sends γ_1 instead of $\|\mathbf{x}\|$, one has the extra advantage of providing the value of γ_1 with a low quantization error, which reduces the overall distortion.

For transmission, it is important that if coefficients and/or atom indices are lost, the decoder can just ignore the lost terms when reconstructing the signal. Therefore, in order to improve error resilience, it would be desirable that the quantizer for a given γ_m be independent of the quantized values of other γ_l ($l \neq m$). One way to accomplish this is to use the same quantization rule for all coefficients of the M-term. In this work we achieve that by designing a single quantizer. The same quantizer is applied for $\gamma_m, 1 < m \leq M$, being M the number of decomposition steps. For that purpose one considers that the values to be quantized are drawn from the sample space formed by the superposition of the ones corresponding to the Δ_m ($m \geq 2$). In terms of sample spaces, one has that $\mathcal{S}_\Delta = \bigcup_{m=2}^{M} \mathcal{S}_{\Delta_m}$. Note that, in order to do this, we must ponderate the probability density function $f_\Delta(\delta)$ accordingly. Given a number of MP iterations all iterations are equally likely, therefore, the pdf of Δ is the average of the pdfs of each Δ_m, that is

$$f_\Delta(\delta) = \frac{1}{M-1} \sum_{m=2}^{M} f_{\Delta_m}(\delta_m). \tag{20}$$

5.1. Distortion for an optimal quantizer

In Section 3 it was observed that the RVs of the angles Θ_m can be assumed to be uncorrelated. Although the RVs Δ_m and Δ_l may be correlated, when designing a quantizer for Δ drawn from $\mathcal{S}_\Delta = \bigcup_{m=2}^{M} \mathcal{S}_{\Delta_m}$ the assumption that $e_q(\Delta_m)$ and $e_q(\Delta_l)$ (where $e_q(\Delta_m) = \Delta_m - Q[\Delta_m]$ and $m \neq l$) are uncorrelated is reasonable. It is also reasonable to assume that $e_q(\Delta_m)e_q(\Delta_l)$ and $\langle \mathbf{g}_{i(m)}, \mathbf{g}_{i(l)} \rangle$ are uncorrelated. In addition, due to the invariant nature of MP angle statistics, it is possible to infer that the expected value of $\langle \mathbf{g}_{i(m)}, \mathbf{g}_{i(l)} \rangle$ is invariant. More specifically, we consider that $E[\langle \mathbf{g}_{i(m)}, \mathbf{g}_{i(l)} \rangle] = c$, i.e., it is constant. Applying these assumptions to the second term of the right hand side of Eq. (19) yields

$$\frac{\gamma_1^2}{N} \left\{ \sum_{m=2}^{M} \sum_{\substack{l=2 \\ l \neq m}}^{M} E[e_q(\Delta_m) e_q(\Delta_l) \langle \mathbf{g}_{i(m)}, \mathbf{g}_{i(l)} \rangle] \right\}$$

$$= (M-2) E[e_q(\Delta)] \sum_{m=2}^{M} E[e_q(\Delta_m)] c. \tag{21}$$

An optimal quantizer for Δ should be an unbiased estimate of Δ, that is, $E[e_q(\Delta)] = 0$ [37]. This makes the expression in Eq. (21) to vanish. As a result Eq. (19) becomes

$$E[d_M^2 | \gamma_1] = \frac{\gamma_1^2}{N} \sum_{n=2}^{M} E[(\Delta_m - Q[\Delta_m])^2]. \tag{22}$$

Because the same $Q[\cdot]$ applies to all Δ_m, $2 \leq m \leq M$ and $f_\Delta(\delta)$ is given by Eq. (20), then

$$E[d_M^2 | \gamma_1] = \frac{\gamma_1^2 (M-1)}{N} E[(\Delta - Q[\Delta])^2], \tag{23}$$

where the term $M-1$ multiplying the integral takes into account the contribution of the $M-1$ coefficients. In addition, it should be highlighted that no restriction is applied to the number of decomposition steps M and Eq. (23) applies as well for small and large values of M. Eq. (23) means that the distortion of the quantized MP decomposition given its first coefficient (γ_1) is equivalent to the quantization distortion of Δ. This random variable is given by the union of the random variables Δ_m that correspond to the MP coefficients normalized by γ_1. Therefore, if the same quantization rule is applied to all the coefficients in M-terms then one can minimize the quantization distortion by designing the optimal "mean square", or Lloyd–Max quantizer (LMQ) [37] for Δ.

5.2. Lloyd–Max quantizer design

In order to design a Lloyd–Max quantizer (LMQ) [37] for Δ we have to minimize the expression in Eq. (23), that can be written as the following integral:

$$E[d_M^2 | \gamma_1] = \frac{\gamma_1^2 (M-1)}{N} \int (\delta - Q[\delta])^2 f_\Delta(\delta)\, d\delta, \text{ with} \tag{24}$$

$$f_\Delta(\delta) = \frac{1}{M-1} \sum_{m=2}^{M} f_{\Delta_m}(\delta_m),$$

with

$$\Delta_m = \tan(\Theta_1) \left[\prod_{i=2}^{m-1} \sin(\Theta_i) \right] \cos(\Theta_m). \tag{25}$$

The reconstruction levels and thresholds of the L-level or b_{coef} bits ($L = 2^{b_{\text{coef}}}$ levels) LMQ are calculated using an iterative algorithm as the one in [37], with the restriction that they are all constrained to be positive (see discussion following Eq. (11)). An estimate of $f_\Delta(\delta)$ is required for obtaining the LMQ. The $f_{\Delta_m}(\delta_m)$ composing $f_\Delta(\delta)$ (see Eq. (20)) are computed using the model developed in Section 4, whereby the pdfs of MP angles are equal to $f_{\Theta_1}(\theta_1)$. To estimate $f_{\Theta_1}(\theta_1)$, an ensemble of $\#_{\mathcal{D}} N^2$ one-step decompositions of realizations from a Gaussian source was employed. The number of bins employed to estimate $f_{\Theta_1}(\theta_1)$ was varied according to the value of b_{coef}, since for smaller values of b_{coef} one needs less bins for optimizing the quantizer. We used $100 \times 2^{b_{coef}}$ bins for estimating $f_{\Theta_1}(\theta_1)$.

Given that the quantizer design is independent of γ_1; it is sufficient to design quantizers for $\gamma_1 = 1$ and store their copies in both encoder and decoder. Since $f_\Delta(\delta)$ depends on the number of MP terms M, there is a different LMQ for each pair of number of bits per coefficient b_{coef} and M. In order to inform these values to the decoder, the bitstream generated includes a header containing b_{coef}, M and γ_1 quantized with low quantization error. The parameter γ_1 is used to scale the quantizer defined by b_{coef} and M in both coder and decoder, a simple strategy that makes good use of resources and has the extra advantage of

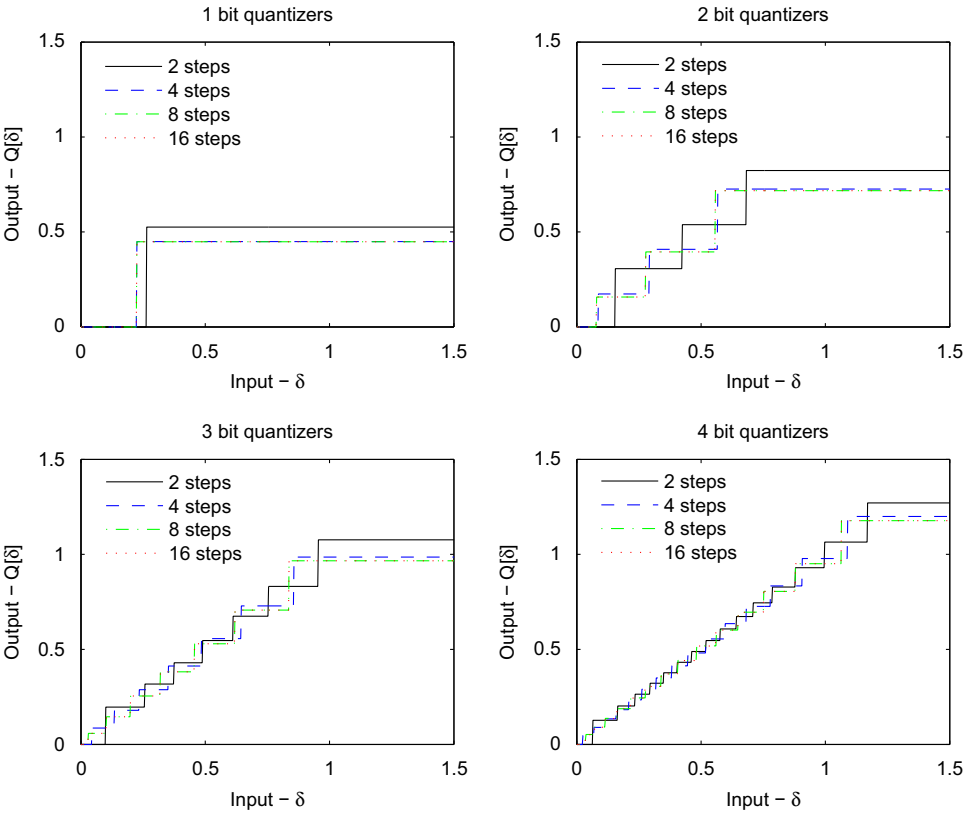

Fig. 14. Coefficient LMQs for a dictionary *GSND*(16,4), with $\gamma_1 = 1$, for 2, 4, 8 and 16 terms.

providing the value of γ_1 with low distortion at the decoder. This approach also avoids the inadequacy of using the same statistical model for the first MP angle as noted in Subsection 4.3 for sources that are not Gaussian.

Fig. 14 shows LMQs obtained for b_{coef} ranging from 1 to 4 bits and M={2, 4, 8, 16}, for a dictionary *GSND*(16,4). One observes that, for a given b_{coef}, the LMQ is almost invariant after a sufficiently large number of terms M. This can be understood through the argument that follows. From the definition of δ_m (see Eq. (18)), and considering that the Θ_i are iid, the pdfs of successive RVs Δ_m get narrower and their averages approach zero as m increases. Therefore, the probability that each Δ_m is small increases as m increases. Since $\Delta = \bigcup_{m=2}^{M} \Delta_m$, the probability of Δ being close to zero also increases with M. Since sufficiently small values of δ are quantized to zero due to the quantizer dead-zone, as a result the distortion due to coefficient quantization in Eq. (22) changes very little after a given M=J. The value of J depends on $f_{\Theta_1}(\theta_1)$ (as the Θ_i are considered to be iid), which in turn depends on the dictionary $\mathcal{D}$. Thus, for practical applications one designs b_{coef} bits LMQs only for the range from 2 to J MP steps. For $M > J$ the quantizer obtained for M=J can be used without major impact. J can be obtained or by observing the quantizer threshold and reconstruction levels or by measuring the quantization distortion as M increases. When their variation from M to M+1 is smaller than a threshold, then J is reached. Note that as b_{coef} increases the quantizer dead-zone shrinks, thus reducing the coefficient range that is mapped to zero. This implies that J also depends on b_{coef}.

6. Comparison to the state of the art

The pair (M,b_{coef}) (number of terms and quantization levels $L = 2^{b_{\text{coef}}}$) defines the LMQ that is applied to all the coefficients of the M-term. Since for an M-term decomposition one has to encode M atoms and $M-1$ coefficients (γ_1 is encoded as side information in a header), it is easy to find a code such that the data rate of the Lloyd–Max quantized MP decomposition is

$$R = M\lceil \log_2(\#_{\mathcal{D}}) \rceil + (M-1)b_{\text{coef}} + b_{\text{header}}. \tag{26}$$

Given an ensemble of signals from a certain source, one can optimize the overall rate-distortion (RD) performance of the proposed MP quantization method by using the procedure that follows. We start by decomposing each signal of the ensemble using the MP algorithm. Then, for each target rate R one searches a bounded subset of $\mathbb{N}^2$ for the pair (M,b_{coef}) that leads to the lowest average distortion for the ensemble. The (M,b_{coef}) pairs leading to the best RD performance curve for the given source can be stored in both coder and decoder. Then, for transmitting a given signal, the coder simply chooses the pair meeting a desired RD target. In the presented work the RD optimization of the LMQ is done considering just the

Gaussian source, that is, the same set of pairs (M, b_{coef}) are employed independently of the source being considered for coding. When coding different sources it is not necessary to indicate the source being coded, i.e. the same quantizer is employed. It should be noticed that the selection of a (M,b_{coef}) pair strategy can be applied for both off-line and on-line quantization. In addition, this RD optimization could be easily adapted to consider more sophisticated RD tradeoffs, as the one in [23].

The EUQ scheme [18] adjusts the number of quantization levels for each MP coefficient according to an RD estimative. The corresponding matlab code has been kindly provided by the authors of [18] and has been used in our experiments. In this code entropy encoding is applied to the differences between successive quantization indices. In order to minimize the impact of using different codes for the different quantization schemes the same coding strategy was applied to the LMQ in our paper. This was done in order for the differences in coding performance to be due solely to the quantizer and not to the coding strategy. Fig. 15 shows the RD curves of quantized MP expansions originated from three different memoryless iid random sources in $\mathbb{R}^{10}$ (Gaussian, uniform and Gamma) using both LMQ and EUQ for a dictionary *GSND*(128,10). For each distinct source the RD plots are averages over an ensemble of 100 signals. For this experiment LMQs were designed for $(M,b_{\text{coef}}) \in ([1,\ldots,16],[1,\ldots,8])$. The EUQ was set so that its header info has the same length as the one of the LMQs, that is, the second coefficient can use from 1 to 128 quantization levels. It can be seen in Fig. 15 that both quantizers have similar RD performance for all three sources; yet, LMQ has better RD performance than EUQ at low rates. LMQ is also able to work at lower data rates than EUQ.

The EUQ codes each signal with a different rate, i.e., its bit-rate is signal dependent since the quantizers it employs depends on the values of the coefficients in the M-term. Therefore, it is important that we evaluate the ability of the two methods to achieve a given data rate. In order to perform such an evaluation, we analyze their RD plots for individual realizations of a random source. Fig. 16 shows the RD curves of three realizations of a Gaussian source when their MP expansions using a dictionary *GSND*(128,10) are quantized with both the RD optimized LMQ and the EUQ. In Fig. 16 one notes that at rates below 12 bits/sample both methods achieve similar distortion. However, the existence of a larger number of RD points at low rate for LMQ than for EUQ indicates that the LMQ provides a finer and more accurate rate control.

Fig. 17 shows the RD curves for LMQ and EUQ for the Gaussian, uniform and Gamma iid sources in $\mathbb{R}^{64}$ using the four-phase Gabor dictionary, see Eq. (16). For that purpose the LMQs were designed with $b_{\text{coef}} \in [1,\ldots,6]$. For each distinct source the results are averages over an ensemble of 200 signals. For instance, note that the coding of these signals employ a pair (M, b_{coef}) that ranges from (1,0) at the lower rate, (32, 4) at 8 bits/sample, to (56, 6) at 16 bits/sample. The decompositions quantized with EUQ require larger bit-rates because the bit allocation employed in [18] fails for dictionaries that have large $\Theta(D)$ (as is often the case in spaces of high dimension). In order to make a fairer comparison with LMQ, and thus better assess the proposed MP angles model, we have introduced a small improvement to EUQ. We allow the

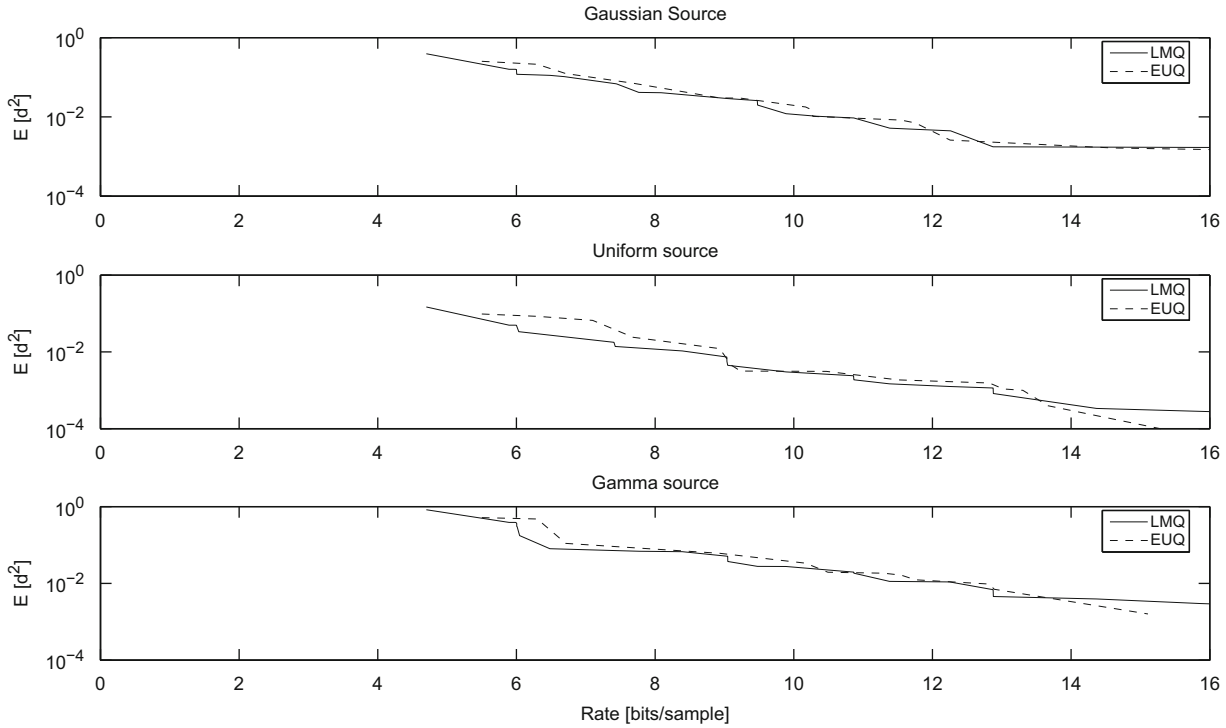

Fig. 15. LMQ and EUQ RDs for three different random sources using the *GSND*(128,10) dictionary.

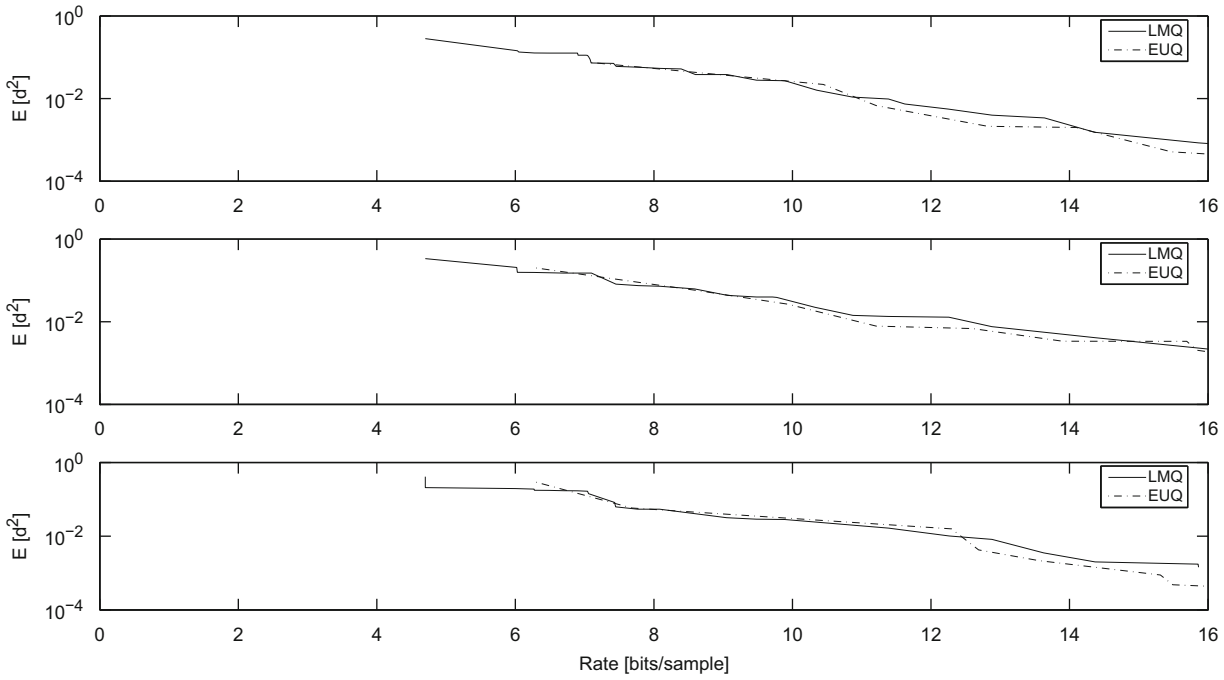

Fig. 16. LMQ compared to the EUQ for the *GSND*(128,10) dictionary—RD curves for three different signals drawn from a Gaussian source.

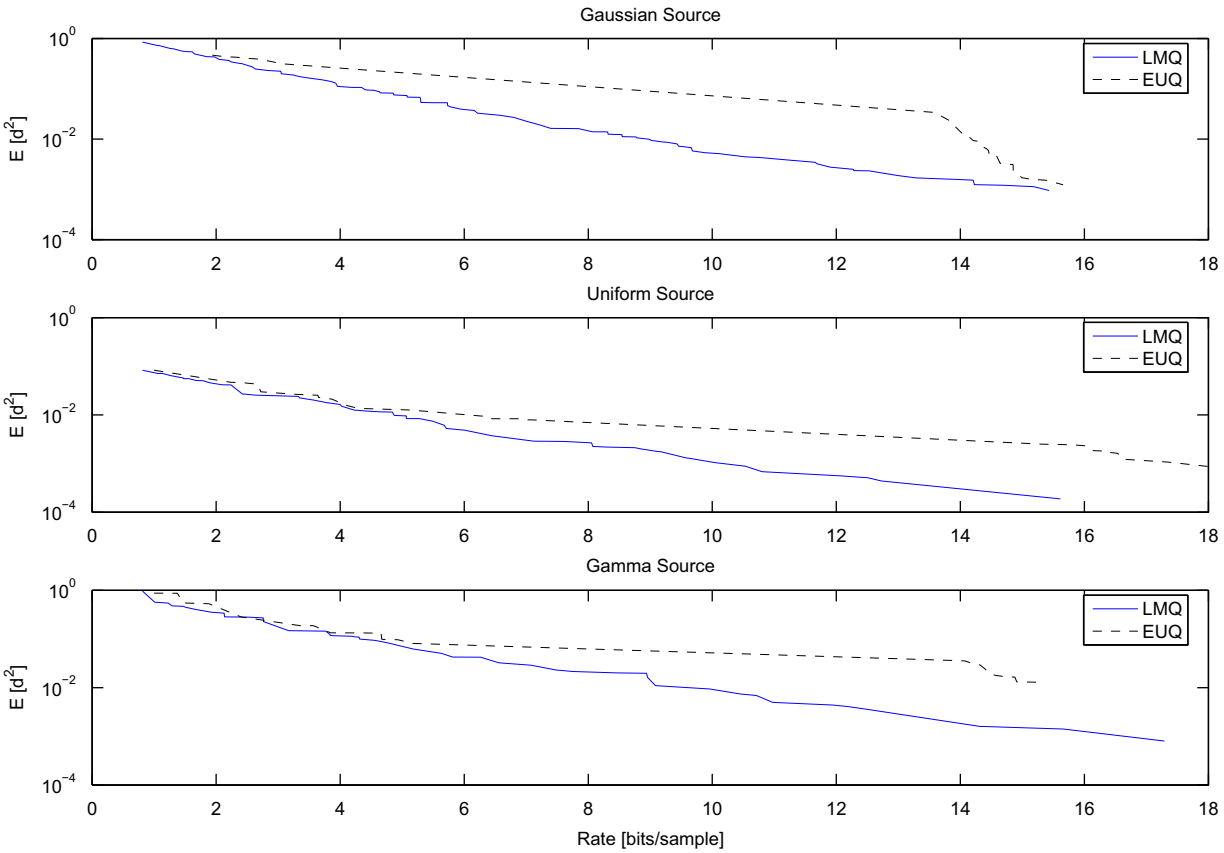

Fig. 17. LMQ and EUQ RDs for three different random sources using the four-phase Gabor dictionary in $\mathbb{R}^{64}$.

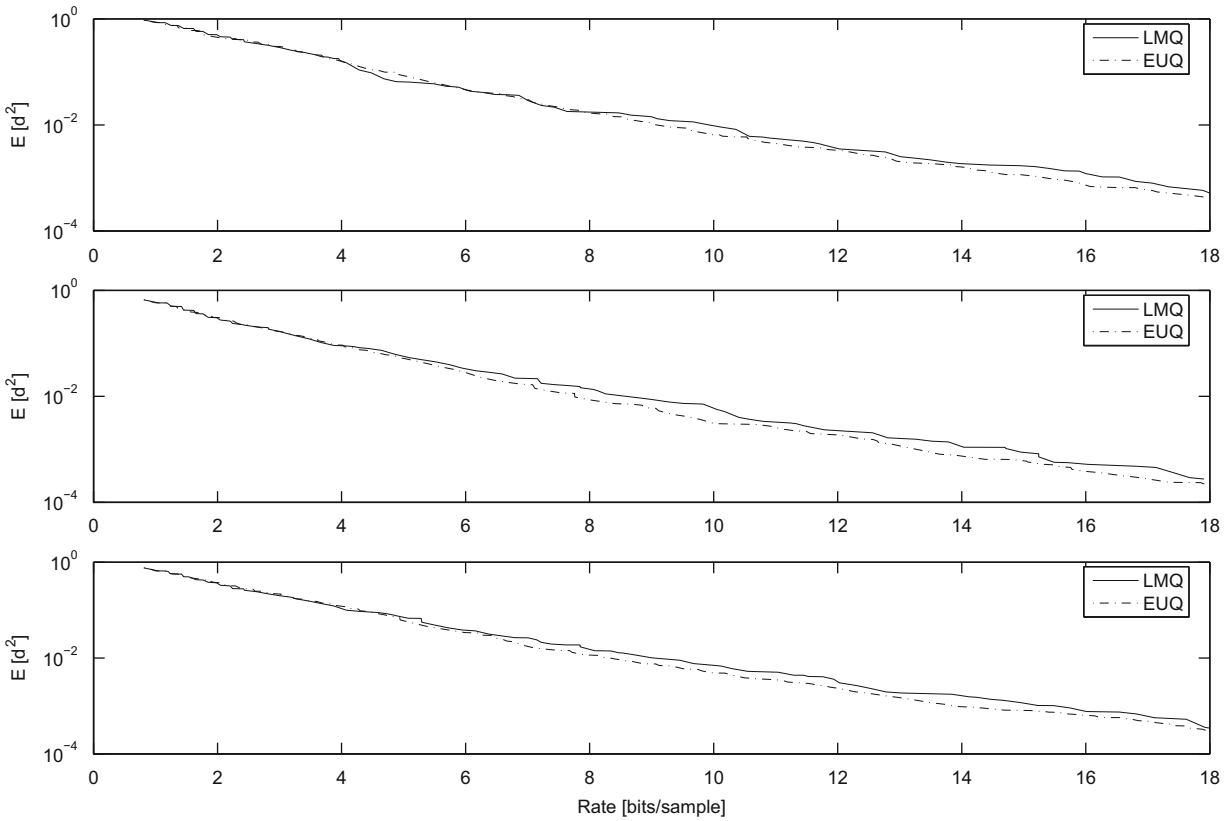

Fig. 18. LMQ compared to the EUQ for the four phases Gabor dictionary in $\mathbb{R}^{64}$—RD curves for three different signals drawn from a Gaussian source.

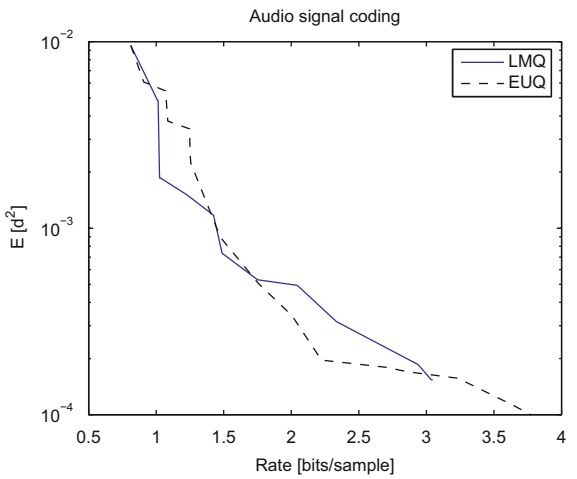

Fig. 19. Rate × Distortion performance for the quantization of the MP decomposition of an audio signal using both LMQ and EUQ for the 4 phases Gabor dictionary in $\mathbb{R}^{64}$.

EUQ bitstream to be truncated after coding any given number of terms in order to provide more accurate rate control. That is the bit-allocation scheme of the EUQ is combined with the truncation of the bitstream that it generates in order to stop coding after any given number of MP steps, what indeed allows for a more precise rate-distortion control. Fig. 18 presents the RD plots of both LMQ and the modified EUQ for three realizations of the random Gaussian source when using the Gabor dictionary of four phases in $\mathbb{R}^{64}$. The decompositions use a total of 100 terms. The LMQs employed to obtain these graphs were designed for $(M,b_{\text{coef}}) \in ([1,\ldots,64],[1,\ldots,8])$. The EUQ was set to allow the quantization of the second coefficient using from 1 to 256 bits. In Fig. 18 one observes that both the "truncated" EUQ and the LMQ have similar RD performance at low bit rates.

Some experiments where also held on real-life signals. We present the results obtained when coding pieces of an audio signal, with both LMQ and EUQ. In this experiment, the audio signal is divided into non-overlapping blocks of 64 samples each and bit-rate is allocated for each individual block independently of other blocks. The results are shown in Fig. 19 where one can observe that the LMQ and EUQ have similar performances indicating that the quantizers designed by the proposed approach may also be valid for correlated sources. Similar results were obtained for x-ray images.

7. Conclusion

When applying the matching pursuit for signal coding, the coefficients of the obtained decompositions need to be quantized. We have focussed on the design of off-loop

quantizers for those coefficients, that is, first the decomposition is obtained and then it is quantized. However, in order for designing quantizers for those coefficients an appropriate statistical model in required. As an alternative for such a statistical model, we studied the statistics of the angles in matching pursuit decompositions.

The empirical analysis of the angle between the residue and the atom selected in matching pursuit iterations led to the conjecture that these angles may be statistically modeled as independent and identically distributed. Therefore, they can approximately be considered as being statistically invariant with respect to the decomposition iteration number. In addition, since matching pursuit residues tend to be chaotic, they do not have any preferred orientation in signal space, thus resembling a memoryless white Gaussian signal source. As a consequence, we considered estimating the statistics of angles between the residuals and corresponding atoms from the statistics of the angle between the outcomes of a Gaussian iid source and its closest atom. Numerical results indicate that this is indeed a good approximation.

It was also shown that if the dictionary includes at least one orthonormal basis then the matching pursuit has a non-null probability to produce a null residue whenever the number of decomposition steps is greater than or equal to the signal space dimension. Therefore, for such dictionaries the independent identically distributed statistical model must employ two different statistical sets. One set applies whenever the iteration number is smaller than the signal dimension and the other applies when the number of the iteration is greater than or equal to the signal dimension.

The independent and identically distributed statistical model of angles between the residuals and closest atoms in the matching pursuit algorithm was assessed by using it to develop a method to encode MP decompositions based on Lloyd–Max quantizers for matching pursuit coefficients. Their design is mainly based on the estimate of the probability density function of the angle with the closest atom for signals drawn from a white Gaussian signal source. The developed method for encoding MP decompositions was compared to a state-of-the-art off-loop MP decomposition encoding scheme; both encoders were shown to have similar rate-distortion performance. Therefore, the derived Lloyd–Max quantizer validates and shows the effectiveness the proposed statistical model for the MP angles.

Appendix A. Proof of the null residue proposition

First we state some relevant definitions and facts:

1. The MP algorithm is employed to decompose vectors $\mathbf{x}$ from a source whose realizations are a subset of $\mathbb{R}^N$.
2. $\mathcal{D}$ is given by $\mathcal{D}\equiv\{\mathbf{g}_k\}_{k\in\{1,\ldots,\#_\mathcal{D}\}}$ and its elements have unit norms, i.e., $\|\mathbf{g}_k\|=1\forall k\in\{1,\ldots,\#_\mathcal{D}\}$ and $\#_\mathcal{D}$ is finite.
3. All dictionary atoms are different, i.e., $|\langle\mathbf{g}_k,\mathbf{g}_j\rangle|<1$, $\forall j\neq k\in\{1,\ldots,\#_\mathcal{D}\}$.
4. We use $f_\mathcal{X}(\mathbf{y})$ to denote the pdf of the signal source $\mathcal{X}$ and $f_{\mathcal{R}^m_\mathbf{x}}(\mathbf{y})$ to denote the pdf of the m-th MP residue.

Definition 1. The *Voronoi region* or *cell* [36] associated to each dictionary element $\mathbf{g}_k$ is

$$\mathcal{V}_k=\{\mathbf{x}\in\mathbb{R}^N|\langle\mathbf{x},\mathbf{g}_k\rangle>\langle\mathbf{x},\mathbf{g}_j\rangle,j\in\{1,\ldots,\#_\mathcal{D}\}-\{k\}\}.$$

(a) Since $\mathbf{g}_k\neq\mathbf{g}_j$ for $j\neq k$ and $\|\mathbf{g}_k\|=1$, then $\mathcal{V}_k\neq\emptyset>0$, $\forall k\in\{1,\ldots,\#_\mathcal{D}\}$, i.e., $\int_{\mathcal{V}_k}d\mathbf{x}>0$, $\forall k\in\{1,\ldots,\#_\mathcal{D}\}$.
(b) Let $d=\min_{\mathbf{g}_j,\ \mathbf{g}_k\in\mathcal{D},\ j\neq k}\|\mathbf{g}_j-\mathbf{g}_k\|$, then if $\|\mathbf{x}\|<d/2$ then $\mathbf{g}_j+\mathbf{x}\in\mathcal{V}_j$, $\forall\mathbf{g}_j\in\mathcal{D}$.
(c) If $\mathbf{x}\in\mathcal{V}_k$ then $a\mathbf{x}\in\mathcal{V}_k$, $a\in\mathbb{R}^*_+$.
(d) At the m-th MP step, if $\mathbf{r}^{m-1}_\mathbf{x}\in\mathcal{V}_k$ then the MP selects $\mathbf{g}_{i(m)}=\mathbf{g}_k$ i.e., $i(m)=k$, for approximating $\mathbf{r}^{m-1}_\mathbf{x}$.
(e) Let $\mathrm{P}(m,k)=\Pr(\mathbf{r}^{m-1}_\mathbf{x}\in\mathcal{V}_k)$ denote the *probability of the m-th MP residual being inside the Voronoi cell* $\mathcal{V}_k$. Note that

$$\mathrm{P}(1,k)=\int_{\mathcal{V}_k}f_\mathcal{X}(\mathbf{x})\,d\mathbf{x},\ldots,\mathrm{P}(m,k)=\int_{\mathcal{V}_k}f_{\mathcal{R}^{m-1}_\mathbf{x}}(\mathbf{y})\,d\mathbf{y}.$$

Definition 2. Let $\mathcal{B}_Q\subset\mathbb{R}^N$, $\mathcal{B}_Q\equiv\{\mathbf{g}_k\}_{k\in\{1,\ldots,Q\}}$ be a set of Q orthonormal vectors, i.e., $\langle\mathbf{g}_i,\mathbf{g}_j\rangle=\delta_{i,j}$, $\forall i,j\in[1,\ldots,Q]$. $H(\mathcal{B}_Q)$ is defined as the Q-dimensional hyper-plane spanned by $\mathcal{B}_Q$, i.e., $\mathbf{x}\in H(\mathcal{B}_Q)$ if and only if $\mathbf{x}=\sum_{i=1}^{Q}\beta_i\mathbf{g}_i,\mathbf{g}_i\in\mathcal{B}_Q$.

Definition 3. Let $\mathcal{B}_Q$ be a set of Q orthonormal vectors in $\mathbb{R}^N$, and $H(\mathcal{B}_Q)$ as in Definition 2. Given $\alpha>0,\varepsilon>0$ and $\mathbf{g}\in H(\mathcal{B}_Q)$, we define $S_Q(\alpha\mathbf{g},\varepsilon,N,\mathcal{B}_Q)$ as a Q-dimensional *hyper-sphere* of radius ε centered at $\alpha\mathbf{g}$ that is contained in $H(\mathcal{B}_Q)$.

(a) Note that for $\alpha>0$ and $\mathbf{x},\mathbf{g}\in H(\mathcal{B}_Q)$, if $\|\mathbf{x}-\alpha\mathbf{g}\|<\varepsilon$ then $\mathbf{x}\in S_Q(\alpha\mathbf{g},\varepsilon,N,\mathcal{B}_Q)$.
(b) Note that if $\mathcal{B}_Q\subset\mathcal{B}_{Q+1}$ and $\mathbf{g}\in H(\mathcal{B}_Q)$ then $S_Q(\alpha\mathbf{g},\varepsilon,N,\mathcal{B}_Q)\subset S_{Q+1}(\alpha\mathbf{g},\varepsilon,N,\mathcal{B}_{Q+1})$.
(c) $S_Q(\mathbf{0},\varepsilon,N,\mathcal{B}_Q)$ denotes a Q-dimensional hyper-sphere of radius ε centered at the origin.

Using the above definitions, the "null residue proposition" is stated in the theorem below.

Theorem 2. *Let $\mathcal{D}\equiv\{\mathbf{g}_k\}_{k\in\{1,\ldots,\#_\mathcal{D}\}}$ contain an orthonormal basis $\mathcal{B}_N$ of $\mathbb{R}^N$, $\mathcal{B}_N\equiv\{\mathbf{g}_{l_k}\}_{k\in\{1,\ldots,N\}}$, i.e., $\exists\mathcal{I}_N\subset\mathbb{N}$, $\mathcal{I}_N=\{l_1,\ldots,l_N\}$ such that $\langle\mathbf{g}_{l_i},\mathbf{g}_{l_j}\rangle=\delta(i-j)$, for i and j $\in\{1,\ldots,N\}$.*

Let the signal source $\mathcal{X}$ have the following property: $\exists\mathbf{g}_{l_k},l_k\in\mathcal{I}_N$, such that $\exists\alpha_{l_k},\varepsilon_{l_k}>0$ with

$$S_N(\alpha_{l_k}\mathbf{g}_{l_k},\varepsilon_{l_k},N,\mathcal{B}_N)\subset\mathcal{V}_{l_k}\quad\text{and}\quad f_\mathcal{X}(\mathbf{x})>0,\quad\forall\mathbf{x}\in S_N(\alpha_{l_k}\mathbf{g}_{l_k},\varepsilon_{l_k},N,\mathcal{B}_N).\tag{27}$$

Then, there is a non-zero probability for the MP selecting only atoms that belong to $\mathcal{B}_N$ in the first $q\leq N$ steps, that is,

$$\Pr(i(1)\in\mathcal{I}_N,i(2)\in\mathcal{I}_N,\ldots,i(q)\in\mathcal{I}_N)>0.\tag{28}$$

This implies a non-zero probability of the residue being null after the N-th MP iteration, that is,

$$\Pr(\mathbf{r}^N_\mathbf{x}=\mathbf{0})>0.\tag{29}$$

In order to prove this theorem we need some auxiliary results.

Lemma 1. *Let $\mathcal{D}$ be as in Theorem 2. Given $0 \le m < N$, let $\mathcal{B}_{N-m} \subset \mathcal{B}_N$ be an orthonormal set defined by $\mathcal{B}_{N-m} \equiv \{\mathbf{g}_{l_k}\}_{l_k \in \mathcal{I}_{N-m}}$, $\mathcal{I}_{N-m} \subset \mathcal{I}_N$. Let $\mathcal{X}_m$ be a source whose outcomes belong to $H(\mathcal{B}_{N-m})$. This means that if $\mathbf{x} \in \mathcal{X}_m$, then $\mathbf{x} = \sum_{l_i \in \mathcal{I}_{N-m}} \beta_{l_i} \mathbf{g}_{l_i}$. If the source $\mathcal{R}_{\mathbf{x}}^{q-1}$ has the following property: $\exists \mathbf{g}_{l_k}$, $l_k \in \mathcal{I}_{N-m}$, such that $\exists \alpha_{l_k}, \varepsilon_{l_k} > 0$ with*

$$S_{N-m}(\alpha_{l_k}\mathbf{g}_{l_k}, \varepsilon_{l_k}, N, \mathcal{B}_{N-m}) \subset \mathcal{V}_{l_k} \quad \text{and}$$
$$f_{\mathcal{R}_{\mathbf{x}}^{q-1}}(\mathbf{y}) > 0 \quad \forall \mathbf{y} \in S_{N-m}(\alpha_{l_k}\mathbf{g}_{l_k}, \varepsilon_{l_k}, N, \mathcal{B}_{N-m}), \tag{30}$$

Then, if $i(q) = l_k$ then $\forall l_i \in \mathcal{I}_{N-m-1} = \mathcal{I}_{N-m} - \{l_k\}$ there exist α_{l_i} and ε_{l_i} such that

$$f_{\mathcal{R}_{\mathbf{x}}^{q}}(\mathbf{y} | i(q) = l_k) > 0, \ \forall \mathbf{y} \in S_{N-m-1}(\alpha_{l_i}\mathbf{g}_{l_i}, \varepsilon_{l_i}, N, \mathcal{B}_{N-m-1}). \tag{31}$$

That is, if $i(q) = l_k$ then the resulting residue satisfies the assumption in Eq. (30) $\forall l_i \in \mathcal{I}_{N-m-1}$.

Proof.

1. Since $\mathcal{B}_{N-m} = \{\mathbf{g}_{l_1}, \ldots, \mathbf{g}_{l_{N-m}}\}$ is an orthonormal basis of $H(\mathcal{B}_{N-m}) \subset \mathbb{R}^N$, any $\mathbf{x} \in H(\mathcal{B}_{N-m})$ can be expressed as $\mathbf{x} = \sum_{i=1}^{N-m} \gamma_{l_i} \mathbf{g}_{l_i}$. Thus, $\forall \mathbf{x} \in S_{N-m}(\alpha_{l_k}\mathbf{g}_{l_k}, \varepsilon_{l_k}, N, \mathcal{B}_{N-m})$ we have that
$$\mathbf{x} = \alpha_{l_k}\mathbf{g}_{l_k} + \sum_{i=1}^{N-m} \beta_{l_i}\mathbf{g}_{l_i} \text{ and then} \|\mathbf{x} - \alpha_{l_k}\mathbf{g}_{l_k}\|^2 = \sum_{i=1}^{N-m} \beta_{l_i}^2 \le \varepsilon_{l_k}^2. \tag{32}$$
2. If when approximating $\mathbf{x}$ the MP iteration selects $\mathbf{g}_{l_k}$, i.e., $i(q) = l_k$, then the resulting residue is $\mathbf{r}_{\mathbf{x}}^q = \mathbf{x} - \gamma_{l_k}\mathbf{g}_k$. From Eq. (32) it follows that $\gamma_{l_k} = \langle \mathbf{x}, \mathbf{g}_{l_k} \rangle = \alpha_{l_k} + \beta_{l_k}$ then
$$\mathbf{r}_{\mathbf{x}}^q = \sum_{l_i \in \mathcal{I}_{N-m} - \{l_k\}} \beta_{l_i}\mathbf{g}_{l_i} \to \|\mathbf{r}_{\mathbf{x}}^q\| = \sqrt{\sum_{l_i \in \mathcal{I}_{N-m} - \{l_k\}} \beta_{l_i}^2} \le \varepsilon_{l_k}.$$
That is, $\mathbf{r}_{\mathbf{x}}^q \in S_{N-m-1}(\mathbf{0}, \varepsilon_{l_k}, N, \mathcal{B}_{N-m-1})$, where $\mathcal{B}_{N-m-1} = \mathcal{B}_{N-m} - \{\mathbf{g}_{l_k}\}$. Therefore, from Eq. (30) we have that
$$f_{\mathcal{R}_{\mathbf{x}}^q}(\mathbf{y} | i(q) = l_k) > 0, \quad \forall \mathbf{y} \in S_{N-m-1}(\mathbf{0}, \varepsilon_{l_k}, N, \mathcal{B}_{N-m-1}). \tag{33}$$
3. It is a fact that $\forall l_i \in \mathcal{I}_{N-m-1}$ one has that $\mathcal{V}_{l_i} \cap S_{N-m-1}(\mathbf{0}, \varepsilon_{l_k}, N, \mathcal{B}_{N-m-1}) \ne \emptyset$.
   (a) Note that $\mathcal{V}_{l_i} \cap H(\mathcal{B}_{N-m-1}) \ne \emptyset$ and $\mathbf{0} \in \mathcal{V}_{l_i} \cap H(\mathcal{B}_{N-m-1})$.
   (b) Note also that if $\mathbf{x} \in \mathcal{V}_{l_i} \cap H(\mathcal{B}_{N-m-1})$ then $a\mathbf{x} \in \mathcal{V}_{l_i} \cap H(\mathcal{B}_{N-m-1})$.
   (c) Let $\mathbf{x} \in \mathcal{V}_{l_i} \cap H(\mathcal{B}_{N-m-1})$, if $a \le \varepsilon / \|\mathbf{x}\|$ then $a\mathbf{x} \in S_{N-m-1}(\mathbf{0}, \varepsilon_{l_k}, N, \mathcal{B}_{N-m-1})$.
4. For each $l_i \in \mathcal{I}_{N-m-1}$ there exists $S_{N-m-1}(\alpha_{l_i}\mathbf{g}_{l_i}, \varepsilon_{l_i}, N, \mathcal{B}_{N-m-1})$ such that
$$S_{N-m-1}(\alpha_{l_i}\mathbf{g}_{l_i}, \varepsilon_{l_i}, N, \mathcal{B}_{N-m-1}) \cap \mathcal{V}_{l_i} = S_{N-m-1}(\alpha_{l_i}\mathbf{g}_{l_i}, \varepsilon_{l_i}, N, \mathcal{B}_{N-m-1})$$
and
$$S_{N-m-1}(\alpha_{l_i}\mathbf{g}_{l_i}, \varepsilon_{l_i}, N, \mathcal{B}_{N-m-1}) \subset S_{N-m-1}(\mathbf{0}, \varepsilon_{l_k}, N, \mathcal{B}_{N-m-1}). \tag{34}$$
This can be shown by the following arguments:
   a From Definition 1(b) we have that for each $\mathbf{g}_{l_i} \in \mathcal{B}_{N-m-1}$ exists $d > 0$ such that
   $$S_{N-m-1}(\mathbf{g}_{l_i}, d, N, \mathcal{B}_{N-m-1}) \cap \mathcal{V}_{l_i} = S_{N-m-1}(\mathbf{g}_{l_i}, d, N, \mathcal{B}_{N-m-1}). \tag{35}$$
   (b) From Definition 1(c), we know that if Eq. (35) holds then $\forall a > 0$,
   $$S_{N-m-1}(a\mathbf{g}_{l_i}, ad, N, \mathcal{B}_{N-m-1}) \cap \mathcal{V}_{l_i} = S_{N-m-1}(a\mathbf{g}_{l_i}, ad, N, \mathcal{B}_{N-m-1}).$$
   (c) It is known that $\forall \mathbf{y} \in S_{N-m-1}(a\mathbf{g}_{l_i}, ad, N, \mathcal{B}_{N-m-1})$, $\|\mathbf{y}\|$ is such that $|a(1-d)| \le \|\mathbf{y}\| \le |a(1+d)|$.
   (d) Therefore, if we select $a < \varepsilon_{l_k} / (|1+d|)$ then $S_{N-m-1}(a\mathbf{g}_{l_i}, ad, N, \mathcal{B}_{N-m-1}) \subset S_{N-m-1}(\mathbf{0}, \varepsilon_{l_k}, N, \mathcal{B}_{N-m-1})$.
   (e) Therefore, if we select $0 < \alpha_{l_i} < a$ and $0 < \varepsilon_{l_i} < ad$ then Eq. (34) is valid.
5. From Eqs. (33) and (34) we have that $\forall l_i \in \mathcal{I}_{N-m-1}$ there exist α_{l_i} and ε_{l_i} such that
$$f_{\mathcal{R}_{\mathbf{x}}^q}(\mathbf{y} | i(q) = l_k) > 0, \quad \forall \mathbf{y} \in S_{N-m-1}(\alpha_{l_i}\mathbf{g}_{l_i}, \varepsilon_{l_i}, N, \mathcal{B}_{N-m-1}). \qquad \square$$

Lemma 2. *Let $\mathcal{D}$ be as in Theorem 2. Let also $\mathcal{B}_{N-m}$ and the source $\mathcal{R}_{\mathbf{x}}^{q-1}$ be as in Lemma 1. Let $\Pr(i(q+1) = l_i | i(q) = l_k)$ be the probability of $i(q+1) = l_i$ given that $i(q) = l_k$ then*

$$\Pr(i(q+1) = l_i | i(q) = l_k) > 0, \ \forall l_i \in \mathcal{I}_{N-m-1} = \mathcal{I}_{N-m} - \{l_k\} \tag{36}$$

Proof.

1. From Lemma 1 we know that if $i(q) = l_k$ then $\forall l_i \in \mathcal{I}_{N-m-1}$ exists $S_{N-m-1}(\alpha_{l_i}\mathbf{g}_{l_i}, \varepsilon_{l_i}, N, \mathcal{B}_{N-m-1})$ such that $f_{\mathcal{R}_{\mathbf{x}}^q}(\mathbf{y} | i(q) = l_k) > 0$, $\forall \mathbf{y} \in S_{N-m-1}(\alpha_{l_i}\mathbf{g}_{l_i}, \varepsilon_{l_i}, N, \mathcal{B}_{N-m-1})$.
2. Since $S_{N-m-1}(\alpha_{l_i}\mathbf{g}_{l_i}, \varepsilon_{l_i}, N, \mathcal{B}_{N-m-1}) \subset \mathcal{V}_{l_i}$, then $\forall l_i \in \mathcal{I}_{N-m-1}$ we have that
$$\Pr(i(q+1) = l_i | i(q) = l_k) = \int_{\mathcal{V}_{l_i}} f_{\mathcal{R}_{\mathbf{x}}^q}(\mathbf{y} | i(q) = l_k)\, d\mathbf{y}$$
$$\ge \int_{S_{N-m-1}(\alpha_{l_i}\mathbf{g}_{l_i}, \varepsilon_{l_i}, N, \mathcal{B}_{N-m-1})} f_{\mathcal{R}_{\mathbf{x}}^q}(\mathbf{y} | i(q) = l_k)\, d\mathbf{y} > 0. \qquad \square$$

Proof of Theorem 2.

1. Since at each MP step $\mathbf{g}_{i(n)} \perp \mathbf{r}_{\mathbf{x}}^n$, then if from steps 1 to q the atoms selected belong to $\mathcal{B}_N$ we have that $\mathbf{r}_{\mathbf{x}}^q \perp \mathbf{g}_{i(k)}, k \in [1, \ldots, q]$, i.e., $\mathbf{r}_{\mathbf{x}}^q \in H(\mathcal{B}_{N-q}), \mathcal{B}_{N-q} = \mathcal{B}_N - \{\mathbf{g}_{i(1)}, \ldots, \mathbf{g}_{i(q)}\}$. Therefore, if $i(1), i(2), \ldots, i(q) \in \mathcal{I}_N$ then necessarily $i(q+1) \notin \{i(1), \ldots, i(q)\}$. However, one still has to account for all the possible ways how this selection can occur. Therefore, restricting the definition of $\mathcal{I}_{N-q}$ to be $\mathcal{I}_{N-q} = \mathcal{I}_N - \{i(1), \ldots, i(q)\}$, (a particular case of I_{N-m} as defined in Lemma 1) one has that
$$\begin{aligned}
&\Pr(i(1), i(2), \ldots, i(q) \in \mathcal{I}_N) \\
&\quad = \Pr(i(1) \in \mathcal{I}_N, i(2) \in \mathcal{I}_{N-1}, \ldots, i(q) \in \mathcal{I}_{N-(q-1)}) \\
&\quad = \sum_{l_{k(1)} \in \mathcal{I}_N} \mathrm{P}(1, l_{k(1)}) \left\{ \sum_{l_{k(2)} \in \mathcal{I}_{N-1}} \Pr(i(2) = l_{k(2)} | i(1) = l_{k(1)}) \right. \\
&\qquad \left. \times \left[\ldots \left(\sum_{l_{k(q)} \in \mathcal{I}_{N-(q-1)}} \Pr(i(q) = l_{k(q)} | i(q\text{-}1) = l_{k(q-1)}) \right) \right] \right\} > 0.
\end{aligned} \tag{37}$$
2. Now we prove that Eq. (37) is valid for $q \le N$ by induction.
   (a) Note that $S_N(\alpha_{l_k}\mathbf{g}_{l_k}, \varepsilon_{l_k}, N, \mathcal{B}_N) \subset [\mathcal{V}_{l_k} \cap H(\mathcal{B}_N)]$. Therefore, Eq. (30) implies that
   $$\mathrm{P}(1, l_k) = \int_{\mathcal{V}_{l_k} \cap H(\mathcal{B}_N)} f_{\mathcal{X}}(\mathbf{y})\, d\mathbf{y} \ge \int_{S_N(\alpha_{l_k}\mathbf{g}_{l_k}, \varepsilon_{l_k}, N, \mathcal{B}_{N-m})} f_{\mathcal{X}}(\mathbf{y})\, d\mathbf{y} > 0.$$
   Note that for the source considered both Lemmas 1 and 2 are valid. That is, $\forall l_i \in \mathcal{I}_{N-1}, \exists \alpha_{l_i}$ and ε_{l_i} such

that

$$f_{\mathcal{R}_{\mathbf{x}}^1}(\mathbf{y}|i(1)\in\mathcal{I}_N)>0,\quad \forall\mathbf{y}\in S_{N\text{-}1}(\alpha_{l_i}\mathbf{g}_{l_i},\varepsilon_{l_i},N,\mathcal{B}_{N\text{-}1}),$$

and

$$\Pr(i(1)\in\mathcal{I}_N,i(2)\in\mathcal{I}_{N\text{-}1})=\sum_{l_k\in\mathcal{I}_N}\mathrm{P}(1,l_k)\sum_{l_i\in\mathcal{I}_{N\text{-}1}}\Pr(i(2)=l_i|i(1)=l_k)>0.$$

(b) Suppose now that for at least one $l_i\in\mathcal{I}_{N\text{-}(M\text{-}1)}$, $\exists\alpha_{l_i}$ and ε_{l_i} such that

$$f_{\mathcal{R}_{\mathbf{x}}^{M\text{-}1}}(\mathbf{y}|i(M\text{-}1)\in\mathcal{I}_{N\text{-}(M\text{-}2)})>0,$$
$$\forall\mathbf{y}\in S_{N\text{-}(M\text{-}1)}(\alpha_{l_i}\mathbf{g}_{l_i},\varepsilon_{l_i},N,\mathcal{B}_{N\text{-}(M\text{-}1)}),$$

and that Eq. (37) is greater than zero for $q=M$.

i. From Lemma 1, we know that $\forall l_i\in\mathcal{I}_{N\text{-}M}$, $\exists\ \alpha_{l_i}$ and ε_{l_i} such that

$$f_{\mathcal{R}_{\mathbf{x}}^{M}}(\mathbf{y}|i(M)\in\mathcal{I}_{N\text{-}(M\text{-}1)})>0,$$
$$\forall\mathbf{y}\in S_{N\text{-}M}(\alpha_{l_i}\mathbf{g}_{l_i},\varepsilon_{l_i},N,\mathcal{B}_{N\text{-}M}).$$

ii. Therefore, from Lemma 2 we have that

$$\sum_{l_i\in\mathcal{I}_{N\text{-}M}}\Pr(i(M+1)=l_i|i(M))>0. \tag{38}$$

iii. Therefore, if $\Pr(i(1),i(2),\ldots,i(M)\in\mathcal{I}_N)>0$ then $\Pr(i(1),i(2),\ldots,i(M+1)\in\mathcal{I}_N)>0$.

(c) If $i(1),i(2),\ldots,i(N\text{-}1)\in\mathcal{I}_N$ then $\mathcal{I}_1=\mathcal{I}_N\text{-}\{i(1),i(2),\ldots,i(N\text{-}1)\}=\{\hat{l}\}$ and the resulting residue is $\mathbf{r}_{\mathbf{x}}^{N\text{-}1}=\alpha\mathbf{g}_{\hat{l}}$ (that is orthogonal to the previously selected elements). Since $\mathbf{g}_{\hat{l}}\in\mathcal{D}$, the MP makes $i(N)=\hat{l}$, therefore

$$\Pr(i(1),i(2),\ldots,i(N\text{-}1),i(N)\in\mathcal{I}_N)=\Pr(i(1),i(2),\ldots,i(N\text{-}1)\in\mathcal{I}_N)>0.$$

(d) In item (b) is was shown that if Eq. (28) is true for $q=M$ then it is also true for $q=M+1$; in item a) it was verified that Eq. (28) is true for $q=2$; in item c) it was verified that for $q=N$ Eq. (28) equates its value for $q=N$-1 therefore, by induction, Eq. (28) is true for any $q\le N$.

3. Note that the selection $i(N)=\hat{l}$ generates a null residue, therefore

$$\Pr(\mathbf{r}_{\mathbf{x}}^N=\mathbf{0})=\Pr(i(1),i(2),\ldots,i(N\text{-}1)\in\mathcal{I}_N)>0.$$

Corollary 1. *Let $\mathcal{D}$ be as in Theorem 2. If the signals to be decomposed using the MP come from an iid Gaussian source then*

$$\Pr(\mathbf{r}_{\mathbf{x}}^q=\mathbf{0})>0,q=N. \tag{39}$$

Proof. The N-dimensional iid Gaussian source is such that $f_{\mathcal{X}}(\mathbf{x})>0$, $\forall\mathbf{x}\in\mathbb{R}^N$, satisfying the condition in Eq. (27) $\forall\mathbf{g}_{l_k}\in\mathcal{B}_N$. This results in $\Pr(\mathbf{r}_{\mathbf{x}}^N=\mathbf{0})>0$. □

References

[1] S. Mallat, Z. Zhang, Matching pursuits with time-frequency dictionaries, IEEE Trans. Signal Process. 41 (12) (1993) 3397–3415.

[2] S. Mallat, A Wavelet Tour of Signal Processing, Academic Press, USA, 1998.

[3] V.K. Goyal, M. Vetterli, N.T. Thao, Quantized overcomplete expansions in $\mathbb{R}^N$: analysis, synthesis, and algorithms, IEEE Trans. Inf. Theory 44 (1) (1998) 1631.

[4] G. Davis, Adaptive nonlinear approximations, Ph. D. Thesis, New York University, 1994.

[5] L. Lovisolo, M.A.M. Rodrigues, E.A.B. da Silva, P.S.R. Diniz, Efficient coherent decompositions of power systems signals using damped sinusoids, IEEE Trans. Signal Process. 53 (2005) 3831–3846.

[6] H. Krim, D. Tucker, S. Mallat, D. Donoho, On denoising and best signal representations, IEEE Trans. Inf. Theory 45 (7) (1999) 2225–2238.

[7] P. Vera-Candeas, N. Ruiz-Reyes, M. Rosa-Zurera, D. Martinez-Munoz, F. Lopez-Ferreras, Transient modeling by matching pursuits with a wavelet dictionary for parametric audio coding, IEEE Signal Process. Lett. 11 (2004) 349–352.

[8] R. Gribonval, E. Bacry, Harmonic decomposition of audio signals with matching pursuit, IEEE Trans. Signal Process. 51 (2003) 101–111.

[9] R. Heusdens, R. Vafin, W.B. Kleijn, Sinusoidal modeling using psychoacoustic-adaptive matching pursuits, IEEE Signal Process. Lett. 9 (2002) 262–265.

[10] M.M. Goodwin, M. Vetterli, Matching pursuits and atomic signal models based on recursive filters banks, IEEE Trans. Signal Process. 47 (7) (1999) 1890–1902.

[11] S. Jaggi, W.C. Carl, S. Mallat, A.S. Willsky, High resolution pursuit for feature extraction, Appl. Comput. Harmon. Anal. 5 (4) (1998) 428–449.

[12] M.M. Goodwin, Adaptive Signal Models: Theory, Algorithms, and Audio Applications, Kluwer, Boston, USA, 1998.

[13] D.L. Donoho, M. Vetterli, R.A. DeVore, I. Daubechies, Data compression and harmonic analysis, IEEE Trans. Inf. Theory 44 (6) (1998) 2435–2476.

[14] K. Engan, S.O. Aase, J.H. Husoy, Multi-frame compression: theory and design, Elsevier Signal Process. 80 (2000) 2121–2140.

[15] R. Neff, A. Zakhor, Very low bit-rate video coding based on matching pursuits, IEEE Trans. Circuits Syst. Video Technol. 7 (1997) 158–171.

[16] O.K. Al-Shaykh, E. Miloslavsky, T. Nomura, R. Neff, A. Zakhor, Video compression using matching pursuits, IEEE Trans. Circuits Syst. Video Technol. 9 (1997) 123–143.

[17] R. Caetano, E.A.B. da Silva, A.G. Ciancio, Matching pursuits video coding using generalized bit-planes, in: IEEE International Conference on Image Processing, Rochester, NY, USA, 2002.

[18] P. Frossard, P. Vandergheynst, R.M. Figueras I Ventura, M. Kunt, A posteriori quantization of progressive matching pursuit streams, IEEE Trans. Signal Process. 52 (2) (2004) 525–535.

[19] C. De Vleeschouwer, B. Macq, SNR scalability based on matching pursuits, IEEE Trans. Multimedia 2 (4) (2000).

[20] L. Lovisolo, M.P. Tcheou, E.A.B. da Silva, M.A.M. Rodrigues, P.S.R. Diniz, Modeling of electric disturbance signals using damped sinusoids via atomic decompositions and its applications, EURASIP Journal on Applied Signal Processing 2007 (2007), Article ID 29507, 15 pages, doi:10.1155/2007/29507.

[21] R. Neff, A. Zakhor, Modulus quantization for matching-pursuit video coding, IEEE Trans. Circuit Syst. Video Technol. 10 (2000) 895–912.

[22] C. De Vleeschouwer, A. Zakhor, In-loop atom modulus quantization for matching pursuit and its application to video coding, IEEE Trans. Image Process. 12 (2003) 1226–1242.

[23] M. Gharavi-Aikhansari, A model for entropy coding in matching pursuit, in: IEEE International Conference on Image Processing, 1998.

[24] E.A.B. Da Silva, D.G. Sampson, M. Ghanbari, A successive approximation vector quantizer for wavelet transform image coding, IEEE Trans. Image Process. 5 (February 1996).

[25] P. Frossard, P. Vandergheynst, Redundancy in non-orthogonal transforms, in: IEEE International Symposium on Information Theory, June 2001.

[26] Z. Zhang, Matching pursuits, Ph.D. Dissertation, New York University, 1993.

[27] L. Lovisolo, E.A.B. da Silva, Uniform distributions of points on an hyper-sphere with applications to vector bit-plane encoding, IEE Proc. on Vision, Image and Signal Process. 148 (2001) 187–193.

[28] J. Hamkins, K. Zeger, Gaussian source coding with spherical codes, IEEE Trans. Inf. Theory 48 (11) (2002) 2980–2989.

[29] G. Davis, S. Mallat, M. Avellaneda, Adaptive greedy approximations, J. Constr. Approx. 13 (1997) 57–98.

[30] I. Daubechies, Ten Lectures on Wavelets, SIAM, Philadelphia, USA, 1991.

[31] S.E. Ferrando, L.A. Kolasa, N. Kovacevic, Algorithm 820: a flexible implementation of matching pursuit for Gabor functions on the interval, ACM Trans. Math. Software 28 (2002) 337–353.
[32] R. Gribonval, M. Nielsen, Sparse representations in unions of bases, IEEE Trans. Inf. Theory 49 (12) (2003) 3320–3325.
[33] J.H. Conway, N.J.A. Sloane, Sphere Packings, Lattices and Groups, second ed., Springer Verlag, New York, USA, 1993.
[34] E.A.B. da Silva, Wavelets transforms for image coding, Ph.D. Thesis, University of Essex, Essex, England, 1995.
[35] S. Kullback, The Kullback-Leibler distance, The Am. Stat. 41 (1987) 340–341.
[36] A. Gersho, R.M. Gray, Vector Quantization and Signal Compression, Kluwer Academic Publishers, Boston, USA, 1992.
[37] A.K. Jain, Fundamentals of Digital Image Processing, 13th ed., Prentice Hall, Englewood Cliffs, NJ, 1989.